

國立臺灣大學理學院物理學系

碩士論文

Department of Physics

College of Science

National Taiwan University

Master Thesis



可精確解非馬可夫開放系統中之量子邏輯閘最佳化控制

Optimal Control of Quantum Gates in an Exactly Solvable
Non-Markovian Open Quantum Bit System

戴榮身

Tai, Jung-Shen

指導教授：管希聖 博士

Advisor: Goan, His-Sheng, Ph.D.

中華民國 102 年 7 月

July, 2013



國立臺灣大學碩士學位論文
口試委員會審定書

可精確解非馬可夫開放系統中之量子邏輯閘最佳化控制
Optimal Control of Quantum Gates in an Exactly Solvable
Non-Markovian Open Quantum Bit System

本論文係 戴榮身 君 (R00222021) 在國立臺灣大學物理學系、
所完成之碩士學位論文，於民國一〇二年七月十五日承下列考試委員
審查通過及口試及格，特此證明

口試委員：

官希聖

(簽名)

(指導教授)

胡崇德

Handwritten signature

誌謝

能夠通過學位考試，並獲得碩士學位，首先要感謝管希聖老師這兩年來的指導。做為指導教授，管老師並沒有給我們太多的壓力，反而希望我們在研究上能自發性的積極主動。對於學生們提出的疑惑，管老師總是認真負責的解答並給予方向，我很喜歡這種指導方式。同時，管老師在教學上的熱忱和盡責的態度，也讓我相當欽佩。感謝胡崇德老師及蘇正耀老師應允擔任我的學位口試委員，用心審閱我的論文並提供寶貴的建議。另外特別感謝郭華承教授以及XinYu Zhao先生在信件中熱心解答我的問題。

感謝研究室同仁們這兩年的陪伴和砥礪。簡崇欽學長做事嚴謹，但言談不失幽默。黃上瑜學長學養豐富，這兩年教導了我許多與研究有關的技術和知識，對於研究的問題也常有獨到的看法，讓我的觀點不至於太過侷限。張晏瑞學長享受人生的態度令人神往。賴彥佑學長插畫的功力讓人讚嘆。黃嘉賢學長工作時的專心致志，是我要努力的目標。黃斌學長碩士班的工作，是我論文主要的參考。楊存毅是我大學以來的好朋友，我們常常彼此分享，不論是學業或人生。洪長力曾一起合作擔任助教。林冠廷是我研究初期的好夥伴，打下我研究成果的基礎。周宜作為研究室唯一的女生，為研究室帶來了許多活力。另外陳柏文學長、陳建彰學長、萬昭宏學長、楊志偉、李彥賢，以及幾位新進的學弟，都曾有過許多研究上的交流及互動。在此向他們致上由衷的謝意。

我要感謝我的父母，他們開明的教育方式，還有無微不至的照顧和關心，讓我的身心靈都十分健康。還要謝謝姥姥從小到大的愛護，希望妳身體健康，少些病痛，奶奶也是。姊姊小時候是我的玩伴，長大後也十分關心我，祝福妳的事業蒸蒸日上。

我要謝謝我美麗可愛的女友云辰。謝謝妳從大學的時候就一直是我知心的好朋友，我的知音。陪我度過一些不開心的，以及許多快樂的日子。有妳在我身邊，即使面對繁重的研究工作，心裡也十分踏實。期待在未來的日子裡，執子之手，一起寫下屬於我們的故事。

最後要感謝台灣大學，以及台大光音社的朋友們。我在台大六年，參與光音社的活動也差不多有五年的時間，學到了很多，也認識不少一輩子的好朋友。六年前我是個懵懂的高中生，六年後帶著大家的祝福，我完成了碩士班的學業，準備展開人生的新頁。感謝所有愛護我，幫助過我的人，也感謝曾經遭遇的困難與挫折，這些都是我成長的養分，是我生命的一部份。



中文摘要

在本論文中，我們結合由克羅托夫(V. Krotov)發展出來的最佳化控制理論(Optimal control theory)，以及精確推導(exactly derived)得到的主方程式(master equation)，以達成非馬可夫開放量子位元系統(non-Markovian open quantum bit system)中，單一量子位元邏輯閘(single-qubit quantum gate)的建構。我們發現，在適當的系統耗散條件之下，最佳化控制方法可以建構高精準度(fidelity)的量子邏輯閘。我們同時定義了一個重要的物理量: Imp ，用以量化在開放系統中，最佳化控制方法對邏輯閘失誤率(gate error)的修正。藉由 Imp 的定義，我們可以找到一個理想的系統參數範圍，讓最佳化控制的效益最大化。

中文關鍵詞: 最佳化控制、精確解、非馬可夫、開放量子系統、量子位元、量子邏輯閘。



Abstract

In this thesis, we apply the optimal control theory based on the Krotov's method to an exactly derived master equation to find control pulses for single-qubit quantum gate operations under the influence of a non-Markovian environment. High fidelity quantum gates can be achieved for moderate qubit decaying parameters. An important quantity, improvement Imp , is defined to quantify the correction of gate errors due to optimal control iteration for the open system. The desired range of parameters for maximum improvement is found in which the effect of optimal control iteration is maximized.

Keywords: Optimal control, Exact solution, Non-Markovian, Open quantum system, Qubit, Quantum gate.

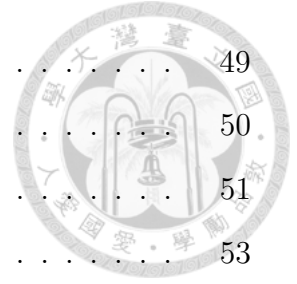


Contents

論文口試委員審定書	i
誌謝	ii
中文摘要	iii
Abstract	iv
1 Introduction	1
2 Non-Markovian Quantum State Diffusion	3
2.1 Overview[1]	3
2.2 Formulation of Non-Markovian Quantum State Diffusion	5
2.2.1 Basic Properties of Coherent States	5
2.2.2 Bargmann States	10
2.2.3 Open Quantum Systems	10
2.2.4 Stochastic Schrödinger Equation	11
2.2.5 Convolution-less Formulation of Non-Markovian Quantum Trajectories	15
2.3 Spin- $\frac{1}{2}$ Examples	17
2.3.1 Measurement-like Interaction (Pure Dephasing Model)	17
2.3.2 Dissipative Model	20



3	Optimal Control Theory	25
3.1	Overview	25
3.2	Optimization Algorithm of a Global Method	26
3.2.1	Control Problem	26
3.2.2	Parameter function and the equivalent representation	26
3.2.3	An iterative algorithm	28
3.2.4	Construction of the parameter function and the improving algorithm	30
3.2.4.1	The sufficient conditions for local extremum	30
3.2.4.2	Realization of the iterative process	33
3.2.5	Reduction of the parameter function	34
3.2.5.1	Linear systems with concave criterion	34
3.2.5.2	Linear systems with quadratic criterion	35
3.3	Optimization Algorithm of a gradient method	35
3.4	Application of OCT to Open Quantum Systems	37
3.4.1	$F(\mathcal{G}(T))$ first order in state	38
3.4.2	$F(\mathcal{G}(T))$ second order in state	40
3.5	Remarks	41
4	Optimal Control of Quantum Gates in Open Systems	43
4.1	Overview	43
4.2	Method	44
4.2.1	Control problem	44
4.2.2	Target	45
4.2.3	Gate error and control update	46
4.2.4	Range of control parameter	47
4.2.5	Initial guess	48
4.3	Results	48



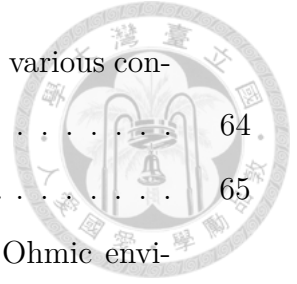
4.3.1	Lorentzian-like spectral density	49
4.3.2	Identity gate	50
4.3.3	Improvement	51
4.3.4	Z-gate	53
4.4	Ohmic spectral density	57
4.4.1	Identity gate	58
4.4.2	Z-gate	60
4.5	Environment suppression ability of optimal control	61
4.5.1	Error correction due to phase shift	61
4.5.2	Conditions for mass improvement	63
4.5.3	Suppression of dissipation	68
5	Conclusion	70
A	Lorentzian spectral density and cavity QED	72
B	Fidelity in Closed and Open Systems	75



List of Figures

4.1	Lorentzian-like correlation function plotted at various conditions. Here $\alpha = 0.01$	50
4.2	Gate error of identity-gate control vs. operation time. Here the environment central frequency coincides with the system transition frequency, <i>i.e.</i> , $\Omega = \omega_0$	51
4.3	The gate error vs. iteration profile and a typical control pulse for identity gate control.	52
4.4	Improvement vs. operation time with $\Omega = \omega_0$ for various conditions.	53
4.5	(a) Gate error vs. iteration profile and (b) a typical control pulse for Z-gate control.	54
4.6	Improvement of Z-gate control in a Lorentzian-like environment under various conditions. Here the values of α and γ are in units of ω_0	56
4.7	Correlation function corresponding to an Ohmic spectral density with $\alpha_o = 0.01$ for various cutoff frequencies.	58
4.8	Plots of identity gate control for various cutoff frequencies, $\alpha_o = 0.01$	59
4.9	Improvement of Z-gate control in a Ohmic environment under various conditions with the Ohmic spectral density.	60
4.10	Comparison of the function $F(s)$ before and after the optimal control. Here $F_0(s)$ denotes the function before the control iteration and $F(s)$ denotes the function after the iteration.	62

4.11	The function $F_0(s)$ in an Lorentzian-like environment under various conditions.	64
4.12	$F_0(s)$ in an Ohmic environment at various cutoff frequency.	65
4.13	The spectral density of a Lorentzian environment and an Ohmic environment. The relative position of the qubit transition frequency ω_0 is shown.	67
4.14	Results of optimal control with a large control range, $ \epsilon(t) \leq 20\omega_0$. . .	69





List of Tables

4.1	Z-gate error under various conditions with a Lorentzian-like spectral density. The value before the arrow denotes the error generated from the ideal closed system control pulse and the value after the arrow denotes the saturate error after the optimization iterations.	54
4.2	Z-gate error under various conditions with an Ohmic spectral density. The value before the arrow denotes the error generated from the ideal closed system control pulse and the value after the arrow denotes the saturate error after the optimization iterations.	60
4.3	Phase difference of various cases before and after the optimal control iteration.	63



Chapter 1

Introduction

Quantum information science and quantum computation has been a hot research field since the pioneering paper of Feynman in 1982 [2]. In quantum information science, the basic element is a quantum bit, or qubit, which is a quantum mechanical analogue to the classical bit in classical computation. A qubit is a quantum two-level system which can be in either the classical computational state, 0 or 1, or the superposition state of both 0 and 1. Superposition, along with other novel properties allowed by quantum mechanics, such as quantum interference and quantum entanglement, enable certain quantum algorithms which are much more powerful than classical algorithms [3, 4].

Experimentally, several practical systems, such as ion traps [5], cold atoms [6], and solid-state devices [7, 8, 9], have shown the potential of physically realizing quantum computation. However, in these systems, the qubit is inevitably coupled to the environment and suffer from dissipation or decoherence. These environment effects destroy the coherence of a qubit or the entanglement between qubits, which is crucial to quantum computation. Up to now, a true large scale quantum computer is still far from reach.

Optimal control theory applied to quantum systems is a powerful tool for calculating the optimal control pulse to minimize/maximize a desired physical quantity. It has also been applied to various systems to obtain control pulses for quantum gate operations

[10, 11, 12, 13]. In this work, we combine a master equation exactly derived by the non-Markovian quantum state diffusion method with the optimal control theory to construct single qubit Z-gates and identity gates.

The structure of this thesis is organized as follows: In Chapter 2, a thorough and detailed derivation of the master equation by the non-Markovian quantum state diffusion is given. A two-level dephasing model and a two-level dissipative model are treated. In Chapter 3, we introduce an optimal control theory based on Krotov [14]. Two optimization algorithms, the global-improvement and the gradient-type are specified for two different definitions of the cost functions. The exact master equation and the optimal control method are combined in Chapter 4 to construct single qubit gates. We discuss cases involving a Lorentzian-like environment and those involving an Ohmic environment. An important concept of improvement is proposed and defined to quantify the correction of error generated by the optimal control iteration for the open quantum system. We found out the conditions where considerable improvements are achieved and discuss the physics behind. Chapter 5 concludes the thesis.



Chapter 2

Non-Markovian Quantum State

Diffusion

2.1 Overview[1]

The dynamics of open quantum systems is very different from that of closed systems. In closed systems, the dynamics is unitary and the evolution of the system state vector follows the Schrödinger equation; or equivalently, the evolution of system density operator follows the Liouville-von Neumann equation,

$$i\hbar\partial_t\rho_t = [H, \rho_t], \quad (2.1)$$

where ρ_t is the density operator and H is the system Hamiltonian. However, in open quantum system the dynamics is no longer unitary but dissipative (or dephasing), and the dynamics is described by the master equation

$$\dot{\rho}_t = \mathcal{L}_t\rho_t \quad (2.2)$$

where \mathcal{L}_t is the super-operator that acts on the reduced system density operator. In almost all cases, the exact equation of Eq. (2.2) cannot be derived or solved analytically. Even numerical simulation is often beyond today's algorithms and computer capacities.

In the Markov limit, the general form of Eq. (2.2) simplifies and reduces to a master equation of Lindblad form

$$\frac{d}{dt}\rho_t = -\frac{i}{\hbar}[H, \rho_t] + \frac{1}{2}\sum_m \left([L_m\rho_t, L_m^\dagger] + [L_m, \rho_t L_m^\dagger] \right), \quad (2.3)$$

where H is the system's Hamiltonian and the terms involve Lindblad operators L_m describe the effect of the environment in the Markov approximation. This approximation is often very useful because it is valid for many physically relevant situations and because analytical or numerical solutions can be found.

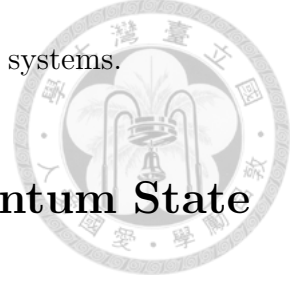
In the past few decades, a breakthrough in solving the Markovian master equation, Eq. (2.3), has been achieved through the discovery of stochastic unravelings of the density operator dynamics. An unraveling is a stochastic Schrödinger equation for stochastic vector states $|\psi_t(z^*)\rangle$, driven by a certain noise z_t such that the density operator is recovered by the ensemble mean of the solutions to the stochastic equation

$$\rho_t = \text{M}[|\psi_t(z^*)\rangle\langle\psi_t(z^*)|],$$

Here $\text{M}[\dots]$ denotes the ensemble mean value over the classical noise z_t according to a certain distribution functional.

In the case of Markovian master equations of Lindblad form Eq. (2.3), the unraveling has been used extensively and provide useful insight into the dynamics of continuously monitored quantum processes. In addition, the unraveling provide an efficient tool for the numerical solution of master equation.[15, 16] It is thus desirable to extend the powerful concept of stochastic unravelings to the more general case of non-Markovian evolution. In the remainder of this chapter we will show how the non-Markovian quan-

tum state diffusion is formulated and give examples on some simple systems.



2.2 Formulation of Non-Markovian Quantum State Diffusion

The derivation uses a coherent state basis for the environmental degrees of freedom [17, 18, 19]. We start from introducing some properties of coherent states [20].

2.2.1 Basic Properties of Coherent States

The coherent state $|z\rangle$ is the eigenstate of the annihilation operator a . Here some basic properties of coherent states are reviewed.

Proposition 1: *If a harmonic oscillator, with Hamiltonian $H = \hbar\omega a^\dagger a$, has as its initial state the coherent state z_0 , then it remains in a coherent state for all times with the oscillating complex amplitude $z(t) = z_0 e^{-i\omega t}$ - i.e. the time-dependent state of the oscillator is given by*

$$|\Psi(t)\rangle = e^{-(i/\hbar)Ht} |z_0\rangle = e^{-i\omega a^\dagger a t} |z_0\rangle = |e^{-i\omega t} z_0\rangle = |z(t)\rangle. \quad (2.4)$$

Proof. We show that $|\Psi(t)\rangle$ is the eigenstate of a with eigenvalue $\alpha(t)$:

$$\begin{aligned} a|\Psi(t)\rangle &= a e^{-i\omega a^\dagger a t} |z_0\rangle \\ &= e^{-i\omega a^\dagger a t} (e^{i\omega a^\dagger a t} a e^{-i\omega a^\dagger a t}) |z_0\rangle \\ &= (e^{-i\omega t} z_0) (e^{-i\omega a^\dagger a t} |z_0\rangle) \\ &= z(t) |\Psi(t)\rangle. \end{aligned}$$

Proposition 2: *The coherent states are minimum uncertainty states: for a mechanical oscillator with position and momentum operators \hat{q} and \hat{p} , respectively,*

$$\Delta q \Delta p = \sqrt{\langle (\hat{q} - \langle \hat{q} \rangle)^2 \rangle} \sqrt{\langle (\hat{p} - \langle \hat{p} \rangle)^2 \rangle} = \frac{1}{2} \hbar \quad (2.5)$$

where the averages are taken with respect to a coherent state.

Proof.

$$\hat{q} = \sqrt{\frac{\hbar}{2m\omega}} (a + a^\dagger),$$

$$\hat{p} = -i\sqrt{\frac{\hbar m\omega}{2}} (a - a^\dagger).$$

Then, for an oscillator in the state $|z\rangle$,

$$\begin{aligned} \langle (\hat{q} - \langle \hat{q} \rangle)^2 \rangle &= \langle \hat{q}^2 \rangle - \langle \hat{q} \rangle^2 \\ &= \frac{\hbar}{2m\omega} \langle z | (a^2 + aa^\dagger + a^\dagger a + a^{\dagger 2}) | z \rangle - \langle \hat{q} \rangle^2 \\ &= \frac{\hbar}{2m\omega} [\langle z | (aa^\dagger - a^\dagger a) | z \rangle + (z + z^*)^2] - \langle \hat{q} \rangle^2 \\ &= \frac{\hbar}{2m\omega} \langle z | [a, a^\dagger] | z \rangle \\ &= \frac{\hbar}{2m\omega}, \end{aligned}$$

where we assume that the state $|z\rangle$ is normalized. Similarly,

$$\langle (\hat{p} - \langle \hat{p} \rangle)^2 \rangle = \frac{\hbar m\omega}{2},$$

Thus,

$$\sqrt{\langle (\hat{q} - \langle \hat{q} \rangle)^2 \rangle} \sqrt{\langle (\hat{p} - \langle \hat{p} \rangle)^2 \rangle} = \frac{1}{2} \hbar.$$

Proposition 3 A normalized coherent state can be expanded in terms of the Fock states $|n\rangle$, $n = 0, 1, 2, \dots$, as

$$|z\rangle = e^{-\frac{1}{2}|z|^2} \sum_{n=0}^{\infty} \frac{z^n}{\sqrt{n!}} |n\rangle. \quad (2.6)$$



Proof. We write

$$|z\rangle = \sum_{n=0}^{\infty} c_n |n\rangle,$$

and substitute this expansion into. Using $a|n\rangle = \sqrt{n}|n-1\rangle$, this gives the relationship

$$\sum_{n=1}^{\infty} c_n \sqrt{n} |n-1\rangle = z \sum_{n=0}^{\infty} c_n |n\rangle.$$

Multiplying on the left by m and using the orthogonality of the Fock states, we have

$$\sum_{n=1}^{\infty} c_n \sqrt{n} \delta_{m,n-1} = z \sum_{n=0}^{\infty} c_n \delta_{m,n},$$

or

$$c_{m+1} \sqrt{m+1} = z c_m.$$

Thus,

$$c_n = \frac{z^n}{\sqrt{n!}} c_0,$$

c_0 is determined by the normalization condition $\langle \alpha | \alpha \rangle = 1$:

$$\begin{aligned} \langle \alpha | \alpha \rangle &= |c_0|^2 \sum_{n,m=0}^{\infty} \frac{z^{*n} z^m}{\sqrt{n!m!}} \langle n | m \rangle \\ &= |c_0|^2 \sum_{n=0}^{\infty} \frac{|z|^{2n}}{n!} \\ &= |c_0|^2 e^{|z|^2}. \end{aligned}$$



Thus,

$$c_0 = e^{-\frac{1}{2}|z|^2},$$

where the arbitrary phase has been chosen so that c_0 is real.

Proposition 4 *The coherent states are not orthogonal; the overlap of the states $|z\rangle$ and $|\zeta\rangle$ is given by*

$$|\langle z|\zeta\rangle|^2 = e^{-|z-\zeta|^2}. \quad (2.7)$$

Note that $|z\rangle$ and $|\zeta\rangle$ are approximately orthogonal when $|z-\zeta|^2$ becomes large.

Proof. Using Proposition 3,

$$\begin{aligned} \langle z|\zeta\rangle &= e^{-\frac{1}{2}|z|^2} e^{-\frac{1}{2}|\zeta|^2} \sum_{n,m=0}^{\infty} \frac{z^{*n}\zeta^m}{\sqrt{n!m!}} \langle n|m\rangle \\ &= e^{-\frac{1}{2}|z|^2} e^{-\frac{1}{2}|\zeta|^2} \sum_{n=0}^{\infty} \frac{(z^*\zeta)^n}{n!} \\ &= e^{-\frac{1}{2}|z|^2} e^{-\frac{1}{2}|\zeta|^2} e^{z^*\zeta}. \end{aligned} \quad (2.8)$$

Then

$$\begin{aligned} |\langle z|\zeta\rangle|^2 &= e^{-|z|^2} e^{-|\zeta|^2} e^{z^*\zeta} e^{z\zeta^*} \\ &= e^{-|z-\zeta|^2}. \end{aligned}$$

Proposition 5 *The coherent states are complete:*

$$\frac{1}{\pi} \int d^2z |z\rangle \langle z| = 1, \quad (2.9)$$

the integration being taken over the entire complex plane.

Proof. From Prop. 3

$$\frac{1}{\pi} \int d^2z |z\rangle \langle z| = \frac{1}{\pi} \int d^2z e^{-|z|^2} \sum_{n,m=0}^{\infty} \frac{z^{*n}z^m}{\sqrt{n!m!}} |n\rangle \langle m|,$$

or, in polar coordinates,

$$\frac{1}{\pi} \int d^2 z |z\rangle \langle z| = \frac{1}{\pi} \sum_{n,m=0}^{\infty} \frac{|n\rangle \langle m|}{\sqrt{n!m!}} \int_0^{\infty} dr e^{-r^2} r^{n+m+1} \int_0^{2\pi} d\phi e^{-i(n-m)\phi},$$

where $z = re^{i\phi}$. The integration over ϕ gives zero unless n is equal to m .

Thus,

$$\frac{1}{\pi} \int d^2 z |z\rangle \langle z| = 2 \sum_{n=0}^{\infty} \frac{|n\rangle \langle n|}{n!} \int_0^{\infty} dr e^{-r^2} r^{2n+1}.$$

After integrating by parts n times,

$$\frac{1}{\pi} \int d^2 z |z\rangle \langle z| = 2 \sum_{n=0}^{\infty} \frac{|n\rangle \langle n|}{n!} \frac{1}{2} n! = \sum_{n=0}^{\infty} |n\rangle \langle n| = I. \quad (2.10)$$

The final step follows from the completeness of the Fock states.

Proposition 6 *The coherent states can be generated from the vacuum state by the action of the certain operator a^\dagger :*

$$|z\rangle = e^{-\frac{1}{2}|z|^2} e^{za^\dagger} |0\rangle. \quad (2.11)$$

Proof. Using $a^\dagger |n\rangle = \sqrt{n+1} |n+1\rangle$, we have

$$\begin{aligned} e^{-\frac{1}{2}|z|^2} e^{za^\dagger} |0\rangle &= e^{-\frac{1}{2}|z|^2} \sum_{n=0}^{\infty} \frac{z^n}{n!} a^{\dagger n} |0\rangle \\ &= e^{-\frac{1}{2}|z|^2} \sum_{n=0}^{\infty} \frac{z^n}{n!} \sqrt{n!} |n\rangle \\ &= e^{-\frac{1}{2}|z|^2} \sum_{n=0}^{\infty} \frac{z^n}{n!} |n\rangle. \end{aligned}$$

This is the expression for the Fock state expansion of the coherent state $|z\rangle$.



2.2.2 Bargmann States

We define a special state called the Bargmann state,

$$||z_\lambda\rangle = e^{z_\lambda a_\lambda^\dagger} |0\rangle, \quad (2.12)$$



which by Eq. (2.11) is just the unnormalized coherent state.

2.2.3 Open Quantum Systems

In the case of an open quantum system. The total system can be divided into the system and the environment. If we consider the environment to be a bosonic oscillator bath, the total Hamiltonian can be written as,

$$H_{\text{tot}} = H + \sum_{\lambda} (g_{\lambda}^* L a_{\lambda}^{\dagger} + g_{\lambda} L^{\dagger} a_{\lambda}) + \sum_{\lambda} \omega_{\lambda} a_{\lambda}^{\dagger} a_{\lambda},$$

where H is the system Hamiltonian, L the coupling operator, and g_{λ} and ω_{λ} are the coupling constant and frequency for each oscillator. a_{λ} and $a_{\lambda'}$ satisfy the canonical commutation relation,

$$[a_{\lambda}, a_{\lambda'}] = \delta_{\lambda\lambda'}.$$

For convenience, we set $\hbar = 1$. In the interaction picture,

$$\begin{aligned} H_{\text{tot}}(t) &= e^{iH_{\text{bath}}t} H_{\text{tot}} e^{-iH_{\text{bath}}t} - H_{\text{bath}} \\ &= H + \sum_{\lambda} (g_{\lambda}^* L a_{\lambda}^{\dagger} e^{i\omega_{\lambda}t} + g_{\lambda} L^{\dagger} a_{\lambda} e^{-i\omega_{\lambda}t}) + \sum_{\lambda} \omega_{\lambda} a_{\lambda}^{\dagger} a_{\lambda}, \end{aligned}$$

where we have used the identity

$$\begin{cases} e^{iH_{\text{bath}}t} a_{\lambda} e^{-iH_{\text{bath}}t} = a_{\lambda} e^{-i\omega_{\lambda}t}, \\ e^{iH_{\text{bath}}t} a_{\lambda}^{\dagger} e^{-iH_{\text{bath}}t} = a_{\lambda}^{\dagger} e^{-i\omega_{\lambda}t}. \end{cases}$$

Short proof.

Let

$$s(t) \equiv e^{iH_{\text{bath}}t} a_\lambda e^{-iH_{\text{bath}}t} = e^{i\sum_\lambda \omega_\lambda a_\lambda^\dagger a_\lambda t} a_\lambda e^{-i\sum_\lambda \omega_\lambda a_\lambda^\dagger a_\lambda t} = e^{i\omega_\lambda a_\lambda^\dagger a_\lambda t} a_\lambda e^{-i\omega_\lambda a_\lambda^\dagger a_\lambda t},$$

$$\frac{ds}{dt} = -i\omega_\lambda s(t),$$

$$\implies s(t) = s(0)e^{-i\omega_\lambda t} = a_\lambda e^{-i\omega_\lambda t}.$$

■

2.2.4 Stochastic Schrödinger Equation

Schrodinger Equation for the Total System (system+environment at zero temperature)

The equation describing the dynamics of the total system is the Schrödinger equation,

$$i\partial_t |\Psi_t\rangle = H_{\text{tot}}(t) |\Psi_t\rangle, \quad (2.13)$$

with the initial condition,

$$|\Psi_0\rangle = |\psi_0\rangle |0_1\rangle |0_2\rangle \cdots |0_\lambda\rangle \cdots, \quad (2.14)$$

which indicates that the system is in the initial state $|\psi_0\rangle$ and the environment is at zero temperature with no excitation in the oscillator states.

We go on to show that the total system state $|\Psi_t\rangle$ can be written as the raveling of the stochastic systems state and the Bragmann states

$$|\Psi_t\rangle = \int \frac{d^2z}{\pi} e^{-|z|^2} |\psi_t(z^*)\rangle ||z\rangle.$$

We introduce the following notations,

$$\begin{cases} d^2 z = d^2 z_1 d^2 z_2 \cdots d^2 z_\lambda \cdots, \\ |z|^2 = \sum_\lambda |z_\lambda|^2, \\ \|z\rangle = \|z_1\rangle \otimes \|z_2\rangle \otimes \cdots \otimes \|z_\lambda\rangle \otimes \cdots. \end{cases}$$



First, $|\Psi_t\rangle$ can be decomposed into the following expansion

$$|\Psi_t\rangle = \sum_{ij} C_{ij} |\phi_i^s\rangle \otimes |\phi_j^{\text{Env}}\rangle. \quad (2.15)$$

Using the resolution of identity, Eq. (2.10), one obtains

$$\begin{aligned} I|\Psi_t\rangle &= |\Psi_t\rangle \\ &= \int \frac{d^2 z}{\pi} e^{-|z|^2} \|z\rangle \langle z| |\Psi_t\rangle \\ &= \sum_{ij} C_{ij} \int \frac{d^2 z}{\pi} e^{-|z|^2} |\phi_i^s\rangle \|z\rangle \langle z| |\phi_j^{\text{Env}}\rangle \\ &= \sum_{ij} C_{ij} b_j \int \frac{d^2 z}{\pi} e^{-|z|^2} |\phi_i^s\rangle \|z\rangle \\ &= \int \frac{d^2 z}{\pi} e^{-|z|^2} \sum_{ij} C_{ij} b_j |\phi_i^s\rangle \|z\rangle, \end{aligned}$$

where $b_j = \langle z| |\phi_j^{\text{Env}}\rangle$ and $\sum_{ij} C_{ij} b_j |\phi_i^s\rangle \equiv |\psi_t(z^*)\rangle$. Thus

$$|\Psi_t\rangle = \int \frac{d^2 z}{\pi} e^{-|z|^2} |\psi_t(z^*)\rangle \otimes \|z\rangle.$$

Also note that,

$$\langle z| |\Psi_t\rangle = \sum_{ij} C_{ij} b_j |\phi_i^s\rangle = |\psi_t(z^*)\rangle.$$

Following Eq. (2.13), we have

$$i\partial_t \langle z | \Psi_t \rangle = \langle z | H_{\text{tot}}(t) | \Psi_t \rangle,$$

$$\partial_t |\psi_t(z^*)\rangle = -iH |\psi_t(z^*)\rangle - iL \sum_{\lambda} g_{\lambda}^* z_{\lambda}^* e^{i\omega_{\lambda} t} |\psi_t(z^*)\rangle - iL^{\dagger} \sum_{\lambda} g_{\lambda} e^{-i\omega_{\lambda} t} \frac{\partial}{\partial z_{\lambda}} |\psi_t(z^*)\rangle, \quad (2.16)$$

where we have made use of the identities

$$\begin{cases} a_{\lambda} \|z_{\lambda}\rangle = z_{\lambda} \|z_{\lambda}\rangle, \\ a_{\lambda}^{\dagger} \|z_{\lambda}\rangle = \frac{\partial}{\partial z_{\lambda}} \|z_{\lambda}\rangle. \end{cases} \quad \Rightarrow \quad \begin{cases} \langle z_{\lambda} | a_{\lambda}^{\dagger} = z_{\lambda}^* \langle z_{\lambda} |, \\ \langle z | a_{\lambda} = \frac{\partial}{\partial z_{\lambda}^*} \langle z |. \end{cases}$$

Defining the random variable and the correlation function

$$z_t^* \equiv -i \sum_{\lambda} g_{\lambda}^* z_{\lambda}^* e^{i\omega_{\lambda} t}, \quad (2.17)$$

$$c(t-s) \equiv \sum_{\lambda} |g_{\lambda}|^2 e^{-i\omega_{\lambda}(t-s)}, \quad (2.18)$$

and using the chain rule

$$\frac{\partial}{\partial z_{\lambda}^*} = \int_0^t ds \frac{\partial z_s^*}{\partial z_{\lambda}^*} \frac{\delta}{\delta z_s^*},$$

one can rewrite Eq. (2.16) as

$$\partial_t |\psi_t(z^*)\rangle = -iH |\psi_t(z^*)\rangle + L z_t^* |\psi_t(z^*)\rangle - L^{\dagger} \int_0^t ds c(t-s) \frac{\delta}{\delta z_s^*} |\psi_t(z^*)\rangle. \quad (2.19)$$

Equation (2.19) is the non-Markovian stochastic Schrodinger equation. It is a stochastic equation since it depends on a stochastic process z_s . The dynamics of the system can be described by quantum trajectory derived from this equation or by the master equation, where the reduced density operator can be recovered by ensemble averaging





the stochastic state vector $\psi_t(z^*)$.

$$\begin{aligned}
\rho_t &= \text{Tr} |\Psi_t\rangle \langle \Psi_t| \\
&= \text{Tr} \int \frac{d^2z}{\pi^N} |z\rangle \langle z| |\Psi_t\rangle \langle \Psi_t| \\
&= \int \frac{d^2z}{\pi^N} e^{-|z|^2} |\psi_t(z^*)\rangle \langle \psi_t(z^*)| \\
&\equiv \text{M} [|\psi_t(z^*)\rangle \langle \psi_t(z^*)|].
\end{aligned} \tag{2.20}$$

For this expression, Eq. (2.20), we regard the coherent state variables z as classical stochastic variables with Gaussian distribution. A simple calculation shows that the stochastic process defined as Eq. (2.17) are realizations of the colored Gaussian processes:

$$\text{M}[z_t] = \text{M}[z_t z_s] = 0, \quad \text{M}[z_t z_s^*] = c(t, s). \tag{2.21}$$

Initial State Consistency

$$\begin{aligned}
|\psi_t(z^*)\rangle|_{t=0} &= \langle z | \Psi_0 \rangle \\
&= |\psi_0\rangle \langle z | 0 \rangle = |\psi_0\rangle.
\end{aligned} \tag{2.22}$$

This result follows directly from Proposition 3 in Sec. 2.2.1. At the initial time $t = 0$, the environmental effect does not come into play, so the initial system state is $|\psi_0\rangle$ regardless of the environment. $|\psi_t(z^*)\rangle|_{t=0} = |\psi_0\rangle$ holds for all configurations of z . The initial state is consistent with 2.14 and the reason that the environment initial state corresponds to vacuum state is justified.

2.2.5 Convolution-less Formulation of Non-Markovian Quantum Trajectories



Stochastic Propagator and O -operator

The last term of Eq. (2.16) depends on the history of the random variable z_s and thus it is in general difficult to manipulate this equation. In certain cases, we can change it into a time-convolutionless form. First, consider Eq. (2.13) and the initial state Eq. (2.14) and also

$$|\Psi_t\rangle = U_t |\Psi_0\rangle. \quad (2.23)$$

So

$$\begin{aligned} |\psi_t(z^*)\rangle &= \langle z | U_t | \psi_0 \rangle |0\rangle \\ &= G_t(z^*) |\psi_0\rangle, \end{aligned} \quad (2.24)$$

where $G_t(z^*) \equiv \langle z | U_t | 0 \rangle$ is the stochastic propagator.

Taking the functional derivative of Eq. (2.24) with respect to z_s , we obtain

$$\begin{aligned} \frac{\delta}{\delta z_s^*} |\psi_t(z^*)\rangle &= \left[\frac{\delta}{\delta z_s^*} G_t(z^*) \right] G_t^{-1}(z^*) |\psi_t(z^*)\rangle \\ &\equiv O(t, s, z^*) |\psi_t(z^*)\rangle, \end{aligned} \quad (2.25)$$

where $O(t, s, z^*) \equiv \left[\frac{\delta}{\delta z_s^*} G_t(z^*) \right] G_t^{-1}(z^*)$ is the O -operator. Substituting this into Eq. (2.16), then we have the time-convolutionless stochastic equation

$$\partial_t |\psi_t(z^*)\rangle = \left(-iH + Lz_t^* - L^\dagger \bar{O}(t, z^*) \right) |\psi_t(z^*)\rangle, \quad (2.26)$$

where

$$\bar{O}(t, z^*) \equiv \int_0^t ds c(t-s) O(t, s, z^*).$$

Consistency Condition

The O -operator equation can be obtained by the following consistency condition

$$\partial_t \frac{\delta |\psi_t(z^*)\rangle}{\delta z_s^*} = \frac{\delta}{\delta z_s^*} \partial_t |\psi_t(z^*)\rangle. \quad (2.27)$$

Combining Eq. (2.27) with Eq. (2.26), we get the following O -operator equation

$$\partial_t O(t, s, z^*) = \left[-iH + Lz_t^* - L^\dagger \bar{O}(t, z^*), O(t, s, z^*) \right] - L^\dagger \frac{\delta \bar{O}(t, z^*)}{\delta z_s^*}.$$

Initial Condition

The initial condition of O can be obtained by taking the Markov limit of the non-Markovian stochastic Schrodinger equation. At the Markov limit, the correlation is δ -correlated

$$c(t-s) = \frac{\gamma}{2} \delta(t-s).$$

So Eq. (2.19) becomes

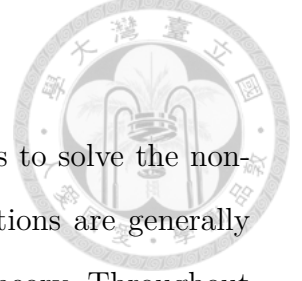
$$\partial_t |\psi_t(z^*)\rangle = -iH |\psi_t(z^*)\rangle + Lz_t^* |\psi_t(z^*)\rangle - \frac{\gamma}{2} L^\dagger \left(\frac{\delta}{\delta z_s^*} |\psi_t(z^*)\rangle \Big|_{t=s} \right). \quad (2.28)$$

Compare Eq. (2.28) with the Markovian quantum state diffusion equation[16]

$$\partial_t |\psi_t(z^*)\rangle = -iH |\psi_t(z^*)\rangle + Lz_t^* |\psi_t(z^*)\rangle - \frac{\gamma}{2} L^\dagger L |\psi_t(z^*)\rangle.$$

We conclude that

$$\frac{\delta}{\delta z_s^*} |\psi_t(z^*)\rangle \Big|_{t=s} = L |\psi_t(z^*)\rangle. \quad (2.29)$$



2.3 Spin- $\frac{1}{2}$ Examples

In this section we use spin- $\frac{1}{2}$ examples to illustrate general methods to solve the non-Markovian QSD equations Eq. (2.19) and Eq. (2.26). These solutions are generally numerical, which illustrate certain features unknown in the Markov theory. Throughout this section $\vec{\sigma}$ denotes the Pauli matrices.

2.3.1 Measurement-like Interaction (Pure Dephasing Model)

Consider a simple model in which $H = (\omega_0/2)\sigma_z$, $L = \lambda\sigma_z$ with λ being a real number parametrizing the strength of the interaction. The harmonic oscillator environment is characterized by its correlation function $\alpha(t-s)$ which is left arbitrary. For this model the stochastic Schrödinger equation reads

$$\partial_t |\psi_t(z^*)\rangle = -iH |\psi_t(z^*)\rangle + \sigma_z z_t^* |\psi_t(z^*)\rangle - \sigma_z \int_0^t ds \alpha(t-s) \frac{\delta}{\delta z_s^*} |\psi_t(z^*)\rangle. \quad (2.30)$$

The corresponding O -operator equation obeys

$$\partial_t O(t, s, z^*) = \left[-iH + \sigma_z z_t^* - \sigma_z \bar{O}(t, z^*), O(t, s, z^*) \right] - \sigma_z \frac{\delta \bar{O}(t, z^*)}{\delta z_s^*}. \quad (2.31)$$

We can immediately infer that the ansatz $O(t, s, z) = \lambda\sigma_z$ satisfy Eq. (2.31) and the initial condition Eq. (2.29). The O -operator is equal to the coupling operator due to the fact that $[H, L] = 0$ and $L = L^\dagger$. In other cases where the system Hamiltonian does not commute with the coupling operator or the coupling operator is not Hermitian, there would be complications.

So the stochastic Schrödinger equation becomes

$$\partial_t |\psi_t(z^*)\rangle = \left(-i\frac{\omega_0}{2}\sigma_z + \lambda\sigma_z z_t^* - \lambda^2 \int_0^t ds c(t-s) \right) |\psi_t(z^*)\rangle. \quad (2.32)$$

Let

$$|\psi_t(z^*)\rangle = \begin{pmatrix} c_1(t) \\ c_2(t) \end{pmatrix}.$$



Then from 2.32 we get the equations of $c_1(t)$ and $c_2(t)$

$$\begin{cases} \dot{c}_1 = -\frac{i\omega}{2}c_1 + \lambda z_t^* c_1 - \lambda^2 \int_0^t c(t-s) dsc_1, \\ \dot{c}_2 = \frac{i\omega}{2}c_2 + -\lambda z_t^* c_2 - \lambda^2 \int_0^t c(t-s) dsc_2. \end{cases} \quad (2.33)$$

Equation (2.33) can be solved straightforwardly to yield

$$\begin{cases} c_1(t) = c_1(0) \exp \left[-\frac{i\omega_0 t}{2} + \lambda \int_0^t z_s^* ds - \lambda^2 \int_0^t dv \int_0^v dsc(v-s) \right], \\ c_2(t) = c_2(0) \exp \left[\frac{i\omega_0 t}{2} - \lambda \int_0^t z_s^* ds - \lambda^2 \int_0^t dv \int_0^v dsc(v-s) \right]. \end{cases} \quad (2.34)$$

The ensemble average of the stochastic vector recovers the density operator

$$\rho_t = M[|\psi_t(z^*)\rangle \langle \psi_t(z^*)|] = M \left[\begin{pmatrix} c_1 c_1^* & c_1 c_2^* \\ c_1^* c_2 & c_2 c_2^* \end{pmatrix} \right],$$

$$\begin{cases} M[c_1 c_1^*] = |c_1(0)|^2 M \left[\exp \left(\lambda \int_0^t ds (z_s^* + z_s) \right) \right] \exp \left(-\lambda^2 F(t) \right), \\ M[c_1^* c_2] = c_1^*(0) c_2(0) M \left[\exp \left(\lambda \int_0^t ds (z_s - z_s^*) \right) \right] \exp \left(i\omega_0 t - \lambda^2 F(t) \right), \\ M[c_1 c_2^*] = c_1(0) c_2^*(0) M \left[\exp \left(\lambda \int_0^t ds (z_s^* - z_s) \right) \right] \exp \left(-i\omega_0 t - \lambda^2 F(t) \right), \\ M[c_2 c_2^*] = |c_2(0)|^2 M \left[\exp \left(-\lambda \int_0^t ds (z_s + z_s^*) \right) \right] \exp \left(-\lambda^2 F(t) \right), \end{cases}$$

where $F(t) \equiv \int_0^t dv \int_0^v ds (c(v-s) + c^*(v-s))$. Making use of the identity[21]



$$\begin{aligned}
& \text{M} \left[\exp \left(\int_0^t ds (f(s)z_s + g(s)z_s^*) \right) \right] \\
&= \exp \left[\int_0^t dv \int_0^t ds (f(v)c^*(v-s)g(s)) \right] \\
&= \exp \left[\int_0^t dv \int_0^v ds (f(v)c^*(v-s)g(s) + f(s)c(s-v)g(v)) \right] \\
&= \exp \left[\int_0^t dv \int_0^v ds (f(v)c^*(v-s)g(s) + f(s)c^*(v-s)g(v)) \right], \tag{2.35}
\end{aligned}$$

where we used $c^*(s-t) = c(t-s)$ from Eq. (2.18) to get the second line in the above equation, we obtain

$$\begin{cases} \text{M} \left[\exp \left(\pm \lambda \int_0^t ds (z_s^* + z_s) \right) \right] = \exp \left[\lambda^2 \int_0^t dv \int_0^v ds (c(v-s) + c^*(v-s)) \right] = \exp \left(\lambda^2 F(t) \right), \\ \text{M} \left[\exp \left(\pm \lambda \int_0^t ds (z_s^* - z_s) \right) \right] = \exp \left[-\lambda^2 \int_0^t dv \int_0^v ds (c(v-s) + c^*(v-s)) \right] = \exp \left(-\lambda^2 F(t) \right). \end{cases}$$

So

$$\begin{aligned}
\rho_t &= \begin{pmatrix} |c_1(0)|^2 & c_1(0)c_2^*(0) \exp(-i\omega_0 t - 2\lambda^2 F(t)) \\ c_1^*(0)c_2(0) \exp(i\omega_0 t - 2\lambda^2 F(t)) & |c_2(0)|^2 \end{pmatrix} \\
&= \begin{pmatrix} \rho_{11}(0) & \rho_{12}(0) (-i\omega_0 t - 2\lambda^2 F(t)) \\ \rho_{21}(0) \exp(i\omega_0 t - 2\lambda^2 F(t)) & \rho_{22}(0) \end{pmatrix}. \tag{2.36}
\end{aligned}$$

Taking the time derivative of Eq. (2.36), we obtain the exact non-Markovian master equation

$$\dot{\rho}_t = -i \frac{\omega_0}{2} [\sigma_z, \rho_t] - \frac{\lambda^2}{2} \int_0^t ds (c(t-s) + c^*(t-s)) [\sigma_z, [\sigma_z, \rho_t]].$$



2.3.2 Dissipative Model

Master Equation

The model considered in this subsection is a simple example with a non-Hermitian coupling operator L . Again the system Hamiltonian $H = \frac{\omega_0}{2}\sigma_z$, but the coupling operator $L = \lambda\sigma_- \equiv \frac{1}{2}\lambda(\sigma_x - i\sigma_y)$ describing spin relaxation. The total Hamiltonian reads

$$H_{\text{tot}} = \frac{\omega_0}{2}\sigma_z + \lambda \sum_k \left(g_k^* \sigma_- a_k^\dagger + g_k \sigma_+ a_k \right) + \sum_k \omega_k a_k^\dagger a_k. \quad (2.37)$$

Hereafter λ will be absorbed into g_k and make λ again the summation index.

$$H_{\text{tot}} = \frac{\omega_0}{2}\sigma_z + \sum_\lambda \left(g_\lambda^* \sigma_- a_\lambda^\dagger + g_\lambda \sigma_+ a_\lambda \right) + \sum_\lambda \omega_\lambda a_\lambda^\dagger a_\lambda. \quad (2.38)$$

We try an ansatz of the form

$$\frac{\delta |\psi_t(z^*)\rangle}{\delta z_s} = f(t, s) \sigma_- |\psi_t(z^*)\rangle \quad (2.39)$$

or namely,

$$O(t, s, z^*) = f(t, s) \sigma_- \quad (2.40)$$

with $f(t, s)$ being a function to be determined.

The consistency condition Eq. (2.27) of the ansatz Eq. (2.40) leads to the condition on $f(t, s)$:

$$\begin{aligned} \partial_t f(t, s) \sigma_- |\psi_t(z^*)\rangle &= \left[-i\frac{\omega_0}{2}\sigma_z - F(t)\sigma_+\sigma_-, f(t, s)\sigma_- \right] |\psi_t(z^*)\rangle \\ &= [i\omega_0 + F(t)] f(t, s) \sigma_- |\psi_t(z^*)\rangle \end{aligned} \quad (2.41)$$

where

$$F(t) \equiv \int_0^t c(t-s) f(t, s) ds.$$

Hence, if $\sigma_- |\psi_t(z^*)\rangle \neq 0$, $f(t, s)$ must satisfy

$$\partial_t f(t, s) = [i\omega_0 + F(t)] f(t, s) \quad (2.42)$$

along with the initial condition $f(s, s) = 1$.

Now we go on to derive the master equation. With the ansatz Eq. (2.40), the stochastic Schrödinger of this model reads

$$\begin{aligned} \partial_t |\psi_t(z^*)\rangle &= -i\frac{\omega_0}{2} \sigma_z |\psi_t(z^*)\rangle + z_t \sigma_- |\psi_t(z^*)\rangle - \sigma_+ \int_0^t ds c(t, s) f(t, s) \sigma_- |\psi_t(z^*)\rangle \\ &= \left(-i\frac{\omega_0}{2} \sigma_z + z_t \sigma_- - \sigma_+ \sigma_- F(t) \right) |\psi_t(z^*)\rangle. \end{aligned} \quad (2.43)$$

Let

$$|\psi_t(z^*)\rangle = \begin{pmatrix} c_1 \\ c_2 \end{pmatrix},$$

and we get the differential equations for c_1 and c_2 :

$$\begin{cases} \dot{c}_1 = -i\frac{\omega_0}{2} c_1 - F(t) c_1, \\ \dot{c}_2 = i\frac{\omega_0}{2} c_2 + z_t c_1. \end{cases} \quad (2.44)$$

Solving Eq. (2.44) we have:

$$\begin{cases} c_1(t) = c_1(0) \exp \left[-i\frac{\omega_0}{2} t - \int_0^t ds F(s) \right], \\ c_2(t) = c_1(0) e^{i\frac{\omega_0}{2} t} \int_0^t du z_u \exp \left[-i\omega_0 u - \int_0^u F(s) ds \right] + c_2(0) e^{i\frac{\omega_0}{2} t}. \end{cases}$$

Recovering the density matrix by ensemble averaging the stochastic state vector, we obtain

$$\rho_t = \mathbb{M} [|\psi_t(z^*)\rangle \langle \psi_t(z^*)|] = \begin{pmatrix} \mathbb{M} [c_1 c_1^*] & \mathbb{M} [c_1 c_2^*] \\ \mathbb{M} [c_2 c_1^*] & \mathbb{M} [c_2 c_2^*] \end{pmatrix},$$





$$\begin{cases} M[c_1 c_1^*] = \rho_{11}(0) \exp\left(-\int_0^t [F(s) + F^*(s)] ds\right), \\ M[c_1 c_2^*] = \rho_{12}(0) \exp\left(-i\omega_0 t - \int_0^t F(s) ds\right), \\ M[c_2 c_1^*] = \rho_{21}(0) \exp\left(i\omega_0 t - \int_0^t F^*(s) ds\right), \\ M[c_2 c_2^*] = 1 - \rho_{11}(0) \exp\left(-\int_0^t [F(s) + F^*(s)] ds\right), \end{cases}$$

where the ensemble means of the random variable Eq. (2.21) have been used. Therefore the density matrix is

$$\rho_t = \begin{pmatrix} \rho_{11}(0) \exp\left(-\int_0^t [F(s) + F^*(s)] ds\right) & \rho_{12}(0) \exp\left(-i\omega_0 t - \int_0^t F(s) ds\right) \\ \rho_{21}(0) \exp\left(i\omega_0 t - \int_0^t F^*(s) ds\right) & 1 - \rho_{11}(0) \exp\left(-\int_0^t [F(s) + F^*(s)] ds\right) \end{pmatrix}. \quad (2.45)$$

Taking the time derivative of Eq. (2.45) we get the master equation

$$\begin{aligned} \dot{\rho}_t &= \begin{pmatrix} -(F(t) + F^*(t)) \rho_{11}(t) & (-i\omega_0 - F(t)) \rho_{12}(t) \\ (i\omega_0 - F^*(t)) \rho_{21}(t) & (F(t) + F^*(t)) \rho_{11}(t) \end{pmatrix} \\ &= -\frac{i\omega_0}{2} [\sigma_z, \rho_t] + (F(t) + F^*(t)) \left(\sigma_- \rho_t \sigma_+ - \frac{1}{2} \{ \sigma_+ \sigma_-, \rho_t \} \right) + \left(\frac{F(t) - F^*(t)}{2} \right) [\sigma_+ \sigma_-, \rho_t]. \end{aligned} \quad (2.46)$$

Equation (2.46) is the master equation for the dissipative system. From Eq. (2.42), function $F(t) \equiv \int_0^t ds c(t, s) f(t, s)$ satisfies the

$$\begin{aligned} \dot{F}(t) &= c(t, t) f(t, t) + \int_0^t ds \{ \partial_t [c(t, s)] f(t, s) + c(t, s) \partial_t f(t, s) \} \\ &= c(t, t) + \int_0^t ds \partial_t [c(t, s)] f(t, s) + i\omega_0 F(t) + F^2(t) \end{aligned} \quad (2.47)$$

with the initial condition

$$F(0) = 0.$$

The bath correlation function $c(t, s)$ is left general here without any assumption.

Arbitrary Correlation Function

In the above, we have not assumed the form of the bath correlation function. Suppose a bath correlation function $\alpha(t, s)$ can be expressed as a sum of exponential functions with complex parameters p_j 's and q_j 's.

$$c(t, s) = \sum_j p_j e^{q_j(t-s)} \equiv \sum_j c_j(t, s),$$

$$\Rightarrow F(t) \equiv \int_0^t ds c(t-s) f(t, s) = \sum_j \int_0^t ds c_j(t, s) f(t, s) \equiv \sum_j F_j(t).$$

Then Eq. (2.47) becomes simultaneous equations of $F_j(t)$ with

$$\begin{aligned} \partial_t F_j(t) &= c_j(t, t) f(t, t) + \int_0^t ds \partial_t [c_j(t, s) f(t, s)] \\ &= p_j + \int_0^t ds \{q_j c_j(t, s) f(t, s) + c_j(t, s) [i\omega_0 t + F(t)] f(t, s)\} \\ &= p_j + F_j(t) \left[q_j + i\omega_0 + \sum_{k \neq j} F_k(t) \right] + F_j^2(t) \end{aligned} \quad (2.48)$$

with the initial condition

$$F_j(0) = 0.$$

$F_j(t)$'s can be calculated numerically and thus we can have $F(t)$ by summing the $F_j(t)$'s.

This result implies that if a given correlation function of arbitrary shape can be fit by complex exponential functions to arbitrary precision, we can take the fitting functions as $F_j(t)$'s and calculate the dynamics of the open system associated with such bath correlation function. In general, the error is lowered as we include more fitting terms, but at the same time, the numerical computation also becomes more expensive.

Exponential Decaying Correlation Function (Lorentzian-like Spectral Density)



In the later chapters we often adopt the following phenomenological bath environment correlation function

$$c_l(t-s) = \alpha \frac{\gamma}{2} e^{-\gamma|t-s| - i\Omega(t-s)}. \quad (2.49)$$

This exponential decaying correlation function corresponds to a Lorentzian spectral density when Ω is sufficiently larger than γ . (The reader may refer to Appendix B for a detailed description.) α being a constant characterizes the coupling strength of the system and the environment. γ^{-1} is the finite environmental memory time scale and Markov case emerges in the limit $\gamma \rightarrow \infty$. Ω is the central frequency of the environment spectrum distribution.

With the correlation in Eq. (2.49), the differential equation of $F(t)$ from Eq. (2.48) becomes

$$\partial_t F(t) = -\gamma F(t) + i(\omega_0 - \Omega + \epsilon(t)) F(t) + F(t)^2 + \frac{\alpha\gamma}{2}. \quad (2.50)$$



Chapter 3

Optimal Control Theory

3.1 Overview

Optimal control theory is an extension of variational calculus which is a mathematical optimization method for deriving control policies. In the field of science and technology, the physical system we are interested in often allows some tunable parameters that are crucial to the system dynamics; some external control fields can be applied to increase the controllability of the system. This controllable system can then be controlled to attain a certain goal such as best performance, least energy consumption, or best fidelity in final state control. An objective functional is defined to quantify how good this goal is fulfilled. Optimal control theory determines the control policy that maximizes/minimizes the objective functional.

Various optimal control theories have been proposed in the last few decades [22, 23]. In this chapter, we introduce methods based on the use of an equivalent representation of the objective functional [14, 24]. A global improvement method and a gradient-type method are studied. Their applications to open quantum systems are compared.

3.2 Optimization Algorithm of a Global Method



3.2.1 Control Problem

Consider a state of some system which can be defined by ψ and is controlled by a time-varying variable $\epsilon(t)$, through the equation of motion¹

$$\dot{\psi}(t) = f(\psi, \epsilon, t). \quad (3.1)$$

The initial value of ψ , $\psi(0) = \psi_0$ is fixed. Given the trajectory $\psi(t)$ and the control $\epsilon(t)$, we define a process $w = (\psi(t), \epsilon(t))$ as a pair of histories satisfying Eq. (3.1). We now define the objective functional on the process w :

$$J[w] = F[\psi(T)] + \int_0^T dt f^0[\psi(t), \epsilon(t)]. \quad (3.2)$$

Here $F[\psi(t)]$ and $f^0[\psi(t), \epsilon(t)]$ are general functions that represent the dependence of J on the final and intermediate time values of ψ . We aim to find a process w that minimizes J . (A maximization problem is similar if we change the sign of J .)

3.2.2 Parameter function and the equivalent representation

To proceed we define a equivalent representation, $L[\psi, \epsilon, \Phi]$, of $J[w]$ such that

$$L[\psi, \epsilon, \Phi] \equiv J[\psi, \epsilon], \quad (3.3)$$

$$L[\psi, \epsilon, \Phi] = G[\psi(T), T] - \Phi(0, \psi(0)) - \int_0^T R[\psi(t), \epsilon(t), t] dt, \quad (3.4)$$

where $\Phi(\psi, t)$ is a parameter function whose utility is to reduce the functional problem of minimizing $J[w]$ to a series of elementary problems of maximizing/minimizing some

¹The state ψ (ϵ) can in general be replaced by a vector $\vec{\psi}$ ($\vec{\epsilon}$) if there are more than one state variables (control variables). In that case Eq. (3.1) becomes $\dot{\vec{\psi}} = \vec{f}(\vec{\psi}, \vec{\epsilon}, t)$. Multiplication of vector variables should then be understood as a inner product.

function of state and control.

G is the final-time contribution:

$$G[\psi(T)] = F[\psi(T)] + \Phi(\Psi(T), T). \quad (3.5)$$



R is the intermediate-time contribution:

$$R[\psi(t), \epsilon(t), t] = -f^0[\psi(t), \epsilon(t)] + \frac{\partial \Phi}{\partial t} + \partial_\psi \Phi \cdot f(\psi, \epsilon, t). \quad (3.6)$$

The functions R and G are designed to separate out the dependence of $L[\psi, \epsilon, \Phi]$ on the final time and intermediate time.

It can be shown that for an arbitrary continuously differentiable scalar function Φ and process w , the equivalence of $L[\psi, \epsilon, \Phi]$ and $J[\psi, \epsilon]$ holds. The derivation is as follows:

$$\begin{aligned} & L[w, \Phi] \\ &= G[\psi(T), T] - \Phi(0, \psi(0)) - \int_0^T R[\psi(t), \epsilon(t), t] dt \\ &= F[\psi(T)] + \Phi(t, \psi(t)) \Big|_0^T - \int_0^T \left\{ -f^0[\psi(t), \epsilon(t)] + \frac{\partial \Phi}{\partial t} + \partial_\psi \Phi \cdot f(\psi, \epsilon, t) \right\} dt \\ &= F[\psi(T)] + \Phi(t, \psi(t)) \Big|_0^T - \int_0^T \left\{ -f^0[\psi(t), \epsilon(t)] + \frac{\partial \Phi}{\partial t} + \frac{\partial \Phi}{\partial \psi} \frac{\partial \psi}{\partial t} \right\} dt \\ &= F[\psi(T)] + \Phi(t, \psi(t)) \Big|_0^T - \int_0^T \frac{d\Phi}{dt} dt + \int_0^T f^0[\psi(t), \epsilon(t)] dt \\ &= F[\psi(T)] + \int_0^T f^0[\psi(t), \epsilon(t)] dt \\ &= J[w]. \end{aligned} \quad (3.7)$$

Therefore, minimizing $J[w]$ is equivalent to minimizing $L[w, \Phi]$ for any Φ which can be achieved by separately minimizing $G[\psi(T), T]$ and maximizing $R[\psi(t), \epsilon(t), t]$.

It is convenient to define the function H through the following relation:

$$R(t, \psi, \epsilon) \equiv H\left(t, \psi, \epsilon, \frac{\partial \Phi(t, \psi)}{\partial \psi}\right) + \frac{\partial}{\partial t} \Phi(t, \psi),$$



where

$$H(t, \psi, \epsilon, p) = pf(t, \psi, \epsilon) - f^0(t, \psi, \epsilon).$$

Here $p \equiv \partial \Phi / \partial \psi$. This extra parameterization emphasizes that ψ and $\partial \Phi / \partial \psi$ should be treated as independent variables, with respect to H .

3.2.3 An iterative algorithm

We now turn to our main goal and describe the Krotov iterative method for finding a sequence of process $\{w_s\}$ which monotonically decrease the value of the objective functional $J[w]$. The central idea is that $L[\psi, \epsilon, \Phi]$ coincide with the objective functional $J[\psi, \epsilon]$ regardless of the choice of the function $\Phi(\psi, t)$. So we may construct Φ such that our current estimate of the state history maximizes $L[\psi, \epsilon, \Phi]$. This makes the current state history the worst of all possible histories given such Φ . We then find a new estimate of control $\epsilon(t)$ which minimizes the objective $L[\psi, \epsilon, \Phi]$ with respect to its explicit dependence on control $\epsilon(t)$. The effect of $\epsilon(t)$ on the objective through the change of $\psi(t)$ can only improve it.

We begin with an arbitrary initial guess of control history $\epsilon^{(0)}(t)$ and integrate Eq. (3.1) to get the corresponding state trajectory $\psi^{(0)}(t)$, which constitute together an initial process $w^{(0)}$.

1. Construct the function $\Phi(t, \psi)$ such that the objective functional is a maximum with respect to state trajectory $\psi(t)$ at the process $w^{(0)}$. This is equivalent to the

following tow conditions:

$$R(t, \psi^{(0)}(t), \epsilon^{(0)}(t)) = \min_{\psi} R(t, \psi(t), \epsilon^{(0)}(t)) \quad (3.8)$$

$$G(\psi_T^{(0)}) = \max_{\psi} G(\psi_T). \quad (3.9)$$



The Φ function we construct here makes our current state trajectory worst in minimizing the objective functional (maximizing R , minimizing G). Any change in ψ brought about by a new choice of control $\epsilon(t)$ will only improve the minimization of $J[w]$.

2. For the $\Phi(t, \psi(t))$ constructed above, we find a new control that maximizes $H(t, \psi, \epsilon, (\frac{\partial \Phi}{\partial \psi}))$ and denote it by:

$$\begin{aligned} \tilde{\epsilon}(t, \psi) &= \arg \max_{\epsilon} H\left(t, \psi, \epsilon, \left(\frac{\partial \Phi}{\partial \psi}\right)\right) \\ &= \arg \max_{\epsilon} R(t, \psi(t), \epsilon(t)) \end{aligned} \quad (3.10)$$

The second line follows since R and H is only deferent by $\frac{\partial \Phi}{\partial t}$ that is independent of ϵ . Note that the control $\tilde{\epsilon}(t, \psi)$ is still a function of ψ ; *i.e.*, the control $\tilde{\epsilon}(t)$ should comply with the equation of motion Eq. (3.1). This freedom will be removed in the next step.

3. Requiring that $\tilde{\epsilon}(t, \psi)$ and $\psi(t)$ be consistent with each other through the equation of motion. Equation (3.1) together with the equation $\epsilon = \tilde{\epsilon}(t, \psi)$ provide two equations for the two unknown ϵ and ψ for the next iteration. Sovling these equations self-consistenetly yields the new process $w^{(1)}$.
4. It is now gauranteed that the minimization of the objective has been improved such that $J[w^{(1)}] < J[w^{(0)}]$. This completes the current iteration. The new process $w^{(1)}$ becomes a starting point for the next iteration. The above operations are repeated to achieve further decrease in the objective.



We proceed to prove that indeed $J[w^{(1)}] \leq J[w^{(0)}]$.

$$\begin{aligned}
J[w^{(0)}] - J[w^{(1)}] &= L[w^{(0)}; \Phi] - L[w^{(1)}; \Phi] \\
&= G(\psi_T^{(0)}) - G(\psi_T^{(1)}) + \int_0^T \{R(t, \psi^{(1)}(t), \epsilon^{(1)}(t)) \\
&\quad - R(t, \psi^{(0)}(t), \epsilon^{(0)}(t))\} dt \\
&= \Delta_1 + \Delta_2 + \Delta_3,
\end{aligned} \tag{3.11}$$

where

$$\Delta_1 = G(\psi_T^{(0)}) - G(\psi_T^{(1)}), \tag{3.12}$$

$$\Delta_2 = \int_0^T \{R(t, \psi^{(1)}(t), \epsilon^{(1)}(t)) - R(t, \psi^{(1)}(t), \epsilon^{(0)}(t))\} dt, \tag{3.13}$$

$$\Delta_3 = \int_0^T \{R(t, \psi^{(1)}(t), \epsilon^{(0)}(t)) - R(t, \psi^{(0)}(t), \epsilon^{(0)}(t))\} dt. \tag{3.14}$$

The non-negativeness of Δ_3 and Δ_1 follow from conditions Eqs. (3.8) and (3.9). And Eq. (3.10) ensures the non-negativeness of Δ_2 . This completes the proof.

3.2.4 Construction of the parameter function and the improving algorithm

3.2.4.1 The sufficient conditions for local extremum

The main challenge of implementing the above iterative method lies in the construction of the parameter function Φ that satisfies the conditions Eqs. (3.8) and (3.9). It is proposed that Φ can be constructed in the following form²

$$\Phi(t, \psi) = \chi_i(t)\psi_i + \sigma_{ij}(t) \underbrace{(\psi_i - \psi_i^{(0)})}_{\equiv \Delta\psi_i} \underbrace{(\psi_j - \psi_j^{(0)})}_{\equiv \Delta\psi_j} = \chi_i(t)\psi_i + \sigma_{ij}(t)\Delta\psi_i\Delta\psi_j, \tag{3.15}$$

²For clarity, an indexed notation of vector components is adopted here. $\psi_k = f_k(t, \psi, \epsilon)$, $k = \overline{1, n}$. Here n is the dimension of ψ . Summation convention is implied whenever suitable.

where $\chi_i(t) \equiv \frac{\partial}{\partial \psi_i} \Phi(t, \psi) \Big|_{\psi^{(0)}} = \frac{\partial}{\partial \psi_i} \Phi(t, \psi^{(0)})$. $\sigma_{ij}(t)$ is a matrix function to be determined.

A necessary condition for an extremum of R and G at $w^{(0)} = (\psi^{(0)}, \epsilon^{(0)})$ is the existence of a stationary point. That is:

$$\frac{\partial}{\partial \psi_i} R(t, \psi, \epsilon) \Big|_{w^{(0)}} = 0, \quad (3.16)$$

$$\frac{\partial G(T, \psi_T, \epsilon)}{\partial \psi_{iT}} \Big|_{w^{(0)}} = 0. \quad (3.17)$$

Eq. (3.16) implies that

$$\begin{aligned} \frac{\partial}{\partial \psi_i} R(t, \psi, \epsilon) \Big|_{w^{(0)}} &= \frac{\partial^2 \Phi(t, \psi)}{\partial \psi_i \partial \psi_k} f_k(t, \psi, \epsilon) + \frac{\partial \Phi}{\partial \psi_i} \frac{\partial}{\partial \psi_k} f_k(t, \psi, \epsilon) - \frac{\partial}{\partial \psi_i} f^0(t, \psi, \epsilon) + \frac{\partial}{\partial t} \frac{\partial \Phi(t, \psi)}{\partial \psi_i} \Big|_{w^{(0)}} \\ &= \frac{\partial}{\partial \psi_i} H(t, \psi^{(0)}, \epsilon^{(0)}, \chi) + \frac{\partial^2 \Phi(t, \psi^{(0)})}{\partial \psi_i \partial \psi_k} f_k(t, \psi^{(0)}, \epsilon^{(0)}) + \frac{\partial}{\partial t} \frac{\partial \Phi(t, \psi^{(0)})}{\partial \psi_i} \\ &= \frac{\partial}{\partial \psi_i} H(t, \psi^{(0)}, \epsilon^{(0)}, \chi) + \left(\frac{\partial \psi_k}{\partial t} \frac{\partial}{\partial \psi_k} + \frac{\partial}{\partial t} \right) \frac{\partial \Phi(t, \psi^{(0)})}{\partial \psi_i} \\ &= \frac{\partial}{\partial \psi_i} H(t, \psi^{(0)}, \epsilon^{(0)}, \chi) + \frac{d\chi_i}{dt} = 0. \end{aligned} \quad (3.18)$$

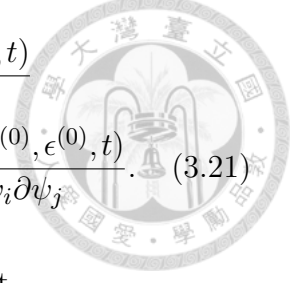
Eq. (3.17) implies that

$$\frac{\partial G(T, \psi^{(0)}(T))}{\partial \psi_i(T)} = \frac{\partial F(\psi^{(0)}(T))}{\partial \psi_i(T)} + \frac{\partial \Phi(T, \psi^{(0)}(T))}{\partial \psi_i(T)} = \frac{\partial F(\psi^{(0)}(T))}{\partial \psi_i(t)} + \chi_i(T) = 0. \quad (3.19)$$

To make the condition sufficient for a relative minimum with respect to ψ of the function $R(t, \psi, \epsilon)$ at $w^{(0)}$, the quadratic form should be non-negative

$$\begin{aligned} d^2 R &= \frac{\partial^2 R}{\partial \psi_i \partial \psi_j} \underbrace{(\psi_i - \psi_i^{(0)})}_{\equiv \Delta \psi_i} \underbrace{(\psi_j - \psi_j^{(0)})}_{\equiv \Delta \psi_j} \Big|_{w^{(0)}} \\ &= \frac{\partial^2 R(t, \psi^{(0)}, \epsilon^{(0)})}{\partial \psi_i \partial \psi_j} \Delta \psi_i \Delta \psi_j. \end{aligned} \quad (3.20)$$

$$\begin{aligned} \frac{\partial^2 R(t, \psi^{(0)}, \epsilon^{(0)})}{\partial \psi_i \partial \psi_j} &= \sigma_{ki} \frac{\partial f_k(\psi^{(0)}, \epsilon^{(0)}, t)}{\partial \psi_j} + \sigma_{kj} \frac{\partial f_k(\psi^{(0)}, \epsilon^{(0)}, t)}{\partial \psi_i} \\ &+ \chi_k \frac{\partial^2 f_k(\psi^{(0)}, \epsilon^{(0)}, t)}{\partial \psi_i \partial \psi_j} + \frac{d\sigma_{ij}}{dt} - \frac{\partial^2 f_0(\psi^{(0)}, \epsilon^{(0)}, t)}{\partial \psi_i \partial \psi_j}. \end{aligned} \quad (3.21)$$



To ensure that the quadratic form Eq. (3.20) be nonnegative, we set

$$\begin{aligned} \frac{\partial^2 R(t, \psi^{(0)}, \epsilon^{(0)})}{\partial \psi_i \partial \psi_j} &= 0, \quad i \neq j, \quad i, j = \overline{1, n} \\ \frac{\partial^2 R(t, \psi^{(0)}, \epsilon^{(0)})}{\partial \psi_i \partial \psi_i} &= \delta_i(t), \quad i = \overline{1, n} \end{aligned} \quad (3.22)$$

where $\delta = \{\delta_i(t)\}$ is a positive vector function.

Similarly, the sufficient condition for a relative minimum of the function $G(T, \psi, \epsilon)$ at $w^{(0)}$ with respect to ψ is ensured by the nonnegativeness of:

$$-d^2 G = -\frac{\partial^2 G(T, \psi^{(0)}(T))}{\partial \psi_i \partial \psi_j} \Delta \psi_i \Delta \psi_j, \quad (3.23)$$

$$\frac{\partial^2 G(T, \psi^{(0)}(T))}{\partial \psi_i \partial \psi_j} = \frac{\partial^2 F(\psi^{(0)}(T))}{\partial \psi_i \partial \psi_j} + \sigma_{ij}(T). \quad (3.24)$$

It is sufficient to set

$$\begin{aligned} -\frac{\partial^2 G(T, \psi^{(0)}(T))}{\partial \psi_i \partial \psi_j} &= 0, \quad i \neq j, \quad i, j = \overline{1, n} \\ -\frac{\partial^2 G(T, \psi^{(0)}(T))}{\partial \psi_i \partial \psi_i} &= \alpha_i, \quad i = \overline{1, n}, \end{aligned} \quad (3.25)$$

where $\alpha = \{\alpha_i\}$ is a positive vector.

By Eqs. (3.22) and (3.25), the matrix σ is determined by solving a linear differential equation with an boundary condition at the right endpoint.

3.2.4.2 Realization of the iterative process



The improvement algorithm reduces to the following sequence of operations:

1. Choose an admissible control history $\epsilon^{(0)}(t)$ and determine the state trajectory $\psi^{(0)}(t)$ by integrating Eq. (3.1) along with the initial condition of the state. Calculate the value of $J[w^{(0)}]$.
2. Integrate eq. (3.18) along with the boundary condition (3.19) to determine the function $\chi(t)$.
3. For convenience, set all the functions $\delta_i(t)$ equal to a non-negative constant δ and all the functions $\alpha_i(t)$ to a non-negative constant α . Determine the matrix $\sigma_{ij}(t)$ by Eqs. (3.22) and (3.25).
4. For the parameter function in accordance with Eq. (3.15) and the matrix function $\sigma_{ij}(t)$ found in the previous step, we found a new control $\tilde{\epsilon}(t, \psi)$ by maximizing $R(t, \psi, \epsilon)$.
5. Find the state trajectory $\psi(t)$ by solving the equation of motion Eq. (3.1) and the control synthesis equation $\epsilon = \tilde{\epsilon}(t, \psi)$ self-consistently. Thus find the new process $w^{(1)} = (\psi^{(1)}, \epsilon^{(1)})$. Calculate the objective functional with respect to this new process $J[w^{(1)}]$.
6. Start a new iteration with the new process $w^{(1)}$ and repeat the iteration. If the functional does not improve, increase δ and α and redo steps 3-5.

Note that the above described algorithm does not sufficiently realize the statement that an absolute minimum of $R(t, \psi, \epsilon^{(0)})$ and an absolute maximum $G(T, \psi(T))$ are attained on the trajectory $\psi^{(0)}$, but rather relative extrema are attained. However, with a suitable choice of δ and α , this algorithm is sufficient to improve the objective functional after every iteration. The drawback is that it ensures only the finding of the

local minimal paths. It is therefore desirable to carry out the iterations with various initial guesses and select the best solution among those obtained.



3.2.5 Reduction of the parameter function

In this section we consider a couple of special problems where the the parameter function, Eq. (3.15), can be simplified or reduced to a first-order function in state.

3.2.5.1 Linear systems with concave criterion

Suppose the equation of motion is linear in state (summation convention)

$$f_i(t, \psi, \epsilon) = a_{ij}(t, \epsilon)\psi_j + b_i(t, u) \quad i = \overline{1, n}. \quad (3.26)$$

The intermediate cost function $f^0(t, \epsilon, \psi)$ and the final time cost $F(\psi(T))$ are concave with respect to ψ

$$\frac{\partial^2 f^0(t, \epsilon, \psi)}{\partial \psi_i^2} \leq 0, \quad \frac{\partial^2 F(\psi)}{\partial \psi_i(T)^2} \leq 0. \quad (3.27)$$

Given the above conditions, we can assign the parameter function $\Phi(t, \psi)$ in the form

$$\Phi(t, \psi) = \chi_i(t)\psi_i,$$

and we have

$$\begin{aligned} R(t, \psi, \epsilon) &= \chi_i(t)b_i(t, \epsilon) + [\chi_i(t)a_{ij}(t, \epsilon)]\psi_j - f^0(t, \epsilon, \psi), \\ G(\psi(T)) &= \chi_i(T)\psi_i - F(\psi(T)). \end{aligned}$$

It is obvious that the function $R(t, \psi, \epsilon)$ is convex with respect to ψ and $G(\psi(T))$ is concave with respect to $\psi(T)$, so Eqs. (3.16) and (3.17) are sufficient for local minimum and maximum respectively on the trajectory $\psi^{(0)}$. Thus in this case, a first-order

parameter function $\Phi(t, \psi)$ suffice and we can get away with the trouble of determining the matrix function $\sigma_{ij}(t)$.



3.2.5.2 Linear systems with quadratic criterion

Suppose the equation is linear in state

$$f_i(t, \psi, \epsilon) = a_{ij}(t, \epsilon)\psi_j + b_i(t, \epsilon) \quad i = \overline{1, n}.$$

The intermediate cost function $f^0(t, \epsilon, \psi)$ and the final time cost $F(\psi(T))$ are quadratic but in general not concave

$$\begin{aligned} f^0(t, \epsilon, \psi) &= a_0(t, \epsilon)\psi^2 + b_0(t, \epsilon)\psi + c_0(t, \epsilon), \\ F(\psi(T)) &= \mu\psi^2 + \nu\psi. \end{aligned}$$

The parameter function, in this case, should be assigned as Eq. (3.15) and the functions $\chi_i(t)$ and $\sigma_{ij}(t)$ should be found by solving their corresponding differential equations. But there exists a favorable fact that since the functions $R(t, \psi, \epsilon)$ and $G(\psi(T))$ are quadratic, Eqs. (3.22) and (3.25) always hold as long as the tuning parameters α and δ are non-negative. There is no need to renew the value of α and δ after every iteration.

3.3 Optimization Algorithm of a gradient method

Here we describe a method of local improvement in terms of the parameter function Φ . The updated process $w^{(1)}$ should be sufficiently close to the original process $w^{(0)}$ such that the sign of the difference of the objective functional is the same as its linear part:

$$\delta J[w^{(0)}] = \delta L = \frac{\partial G(\psi^{(0)}(T))}{\partial \psi} \delta \psi(T) - \int_0^T dt \left(\frac{\partial R}{\partial \psi} \delta \psi(t) + \frac{\partial R}{\partial \epsilon} \delta \epsilon(t) \right), \quad (3.28)$$

where $\delta\psi = \psi - \psi^{(0)}$, $\delta\epsilon = \epsilon - \epsilon^{(0)}$. We require that

$$\frac{\partial}{\partial\psi} R(t, \psi^{(0)}(t), \epsilon^{(0)}(t)) = 0, \quad (3.29)$$

$$\frac{\partial}{\partial\psi} G(\psi^{(0)}(T)) = 0. \quad (3.30)$$



These equations are satisfied by the parameter function in the form $\Phi(t, \psi) = \chi(t)\psi$ where $\chi(t)$ is determined by Eqs. (3.29) and (3.30). Then

$$\delta J[w^{(0)}] = \delta L(w^{(0)}, \Phi) = - \int_0^T dt \frac{\partial R}{\partial \epsilon} \delta \epsilon(t). \quad (3.31)$$

If there exists a function $\delta\epsilon(t)$ such that the integrand in Eq. (3.31) is negative, we can construct an iterative process to improve the objective functional:

1. Find the trajectory $\psi^{(0)}(t)$ by intergrating the equation of motion along with the initial condition using the control $\epsilon^{(0)}$.
2. Find $\chi(t)$ by Eqs. (3.29) and (3.30) which determines the parameter function $\Phi(t, \psi) = \chi(t)\psi$.
3. Set a variation of the control $\delta\epsilon(t)$ which makes the integrand in Eq. (3.31) negative.
4. Solve for $\epsilon^{(1)}(t)$ and $\psi^{(1)}(t)$ self-consistently by the control update equation $\epsilon = \epsilon^{(0)} + \lambda\delta\epsilon$ along with the equation of motion. λ is an arbitrary small positive parameter such that $J[w^{(1)}] < J[w^{(0)}]$ holds.

One of the weak points of this method is the local character of improvement, which is guaranteed only for small variations of the control $\epsilon(t)$. This deficiency is avoided in the global improving method introduced previously.

3.4 Application of OCT to Open Quantum Systems

We now pave the way for applying optimal control theory to constructing quantum gates which will be discussed thoroughly in the next chapter. In open quantum mechanics, the state is described by a density matrix (ensemble of states). The dynamics is described by the master equation along with its initial condition

$$\begin{aligned}\dot{\rho}(t) &= \mathcal{L}\rho(t), \\ \rho(t=0) &= \rho_0,\end{aligned}\tag{3.32}$$

where \mathcal{L} is a superoperator and ρ_t is the density matrix. Here we make a digression by introducing the “vec” operation which transforms a superoperator into an operator and an operator into a column vector:

$$\begin{aligned}\text{vec}(\rho) &= \begin{pmatrix} \rho_{11} \\ \rho_{21} \\ \rho_{12} \\ \rho_{22} \end{pmatrix} = \rho^c = |\rho\rangle\rangle, \\ \text{vec}(AXB) &= (B^T \otimes A) \text{vec}(X), \\ \text{Tr}(A^\dagger B) &= \text{vec}(A)^\dagger \text{vec}(B).\end{aligned}$$

So Eq. (3.32) can be put in the propagator form

$$\begin{aligned}\rho^c(t) &= \mathcal{G}(t)\rho_0^c, \\ \dot{\mathcal{G}}(t) &= \mathcal{L}^c\mathcal{G}(t),\end{aligned}\tag{3.33}$$

$$\mathcal{G}(t=0) = I.\tag{3.34}$$

Here $\mathcal{G}(t)$ is the propagator of ρ_0^c . \mathcal{L}^c is defined such that $\text{vec}(\mathcal{L}\rho) = \mathcal{L}^c\rho^c$.

The vec operation again transforms the propagator $\mathcal{G}(t)$ into a vector. After the operation Eq. (3.33) becomes

$$|\dot{\mathcal{G}}(t)\rangle\rangle = (1 \otimes \mathcal{L}^c) |\mathcal{G}(t)\rangle\rangle = f(t, \mathcal{G}, \epsilon). \quad (3.35)$$



In the state dependent gate control where the density matrix ρ is irrelevant, we treat $|\mathcal{G}(t)\rangle\rangle$ as the state to be controlled and Eq. (3.35) is its equation of motion. Depending on the actual physical system, we are able to insert a control degree of freedom in the evolution operator \mathcal{L} , so \mathcal{L} should be a function of independent variables t and ϵ , $\mathcal{L}(t, \epsilon)$. In the following we discuss two different definition of cost functions and their corresponding optimal iterative processes. The readers may find detailed reasoning for these definitions in Appendix B.

3.4.1 $F(\mathcal{G}(T))$ first order in state

We may define the final-time cost function to be the fidelity multiplied by -1 , such that the minimization of the final time cost is equivalent to the maximization of the fidelity

$$F(\mathcal{G}(T)) = -\frac{1}{N} \text{Re} \left(\text{Tr} \left[O^\dagger \mathcal{G}(T) \right] \right) = -\frac{1}{N} \text{Re} (\langle\langle O | \mathcal{G}(T) \rangle\rangle), \quad (3.36)$$

where O is the “target” and N is the dimension of \mathcal{G} (or O). And the intermediate cost

$$f^0(\epsilon) = \frac{1}{S(t)} (\epsilon - \bar{\epsilon})^2, \quad (3.37)$$

where $S(t)$ is a shape function which also acts as a weighting (for reasons to be revealed shortly).

The intermediate cost may be absurd at first glance but it is actually quite useful in deriving an explicit update rule of the control and in limiting the update rate. These features would be revealed shortly. This problem belongs to the class that has

been discussed in Sec. 3.2.5.1. where a first-order parameter function is enough for improvement. So we may assign the parameter function to be in the following form

$$\Phi = \langle\langle \chi(t) | \mathcal{G}(t) \rangle\rangle + \langle\langle \mathcal{G}(t) | \chi(t) \rangle\rangle = 2\text{Re}(\text{Tr} [\chi(t)\mathcal{G}(t)]). \quad (3.38)$$

And the H function reads

$$\begin{aligned} H &= \langle\langle \chi | 1 \otimes \mathcal{L}^c | \mathcal{G} \rangle\rangle + \langle\langle \mathcal{G} | (1 \otimes \mathcal{L}^c)^\dagger | \chi \rangle\rangle - \frac{1}{S(t)} (\epsilon - \bar{\epsilon})^2 \\ &= 2\text{Re}(\text{Tr} [\chi^\dagger \mathcal{L}^c \mathcal{G}]) - \frac{1}{S(t)} (\epsilon - \bar{\epsilon})^2. \end{aligned} \quad (3.39)$$

The differential equation along with its boundary equation, Eqs. (3.18) and (3.19), for $\chi(t)$ is

$$|\dot{\chi}\rangle\rangle = (1 \otimes \mathcal{L}^c)^\dagger |\chi\rangle\rangle, \quad (3.40)$$

$$|\chi(T)\rangle\rangle = -\frac{1}{2N} |O\rangle\rangle \quad (3.41)$$

In step (4) in Sec 3.2.4.2, the new control is obtained by the necessary condition of a relative maximum of R (or, equivalently, H). That is

$$\frac{\partial H}{\partial \epsilon} = 0, \quad (3.42)$$

$$\frac{\partial^2 H}{\partial \epsilon^2} \leq 0, \quad (3.43)$$

which yields

$$2\text{Re} \left(\text{Tr} \left[\chi(t)^\dagger \frac{\partial \mathcal{L}^c}{\partial \epsilon} \mathcal{G} \right] \right) - \frac{1}{S(t)} (\epsilon - \bar{\epsilon}) = 0, \quad (3.44)$$

$$2\text{Re} \left(\text{Tr} \left[\chi(t)^\dagger \frac{\partial^2 \mathcal{L}^c}{\partial \epsilon^2} \mathcal{G} \right] \right) - \frac{1}{S(t)} \leq 0. \quad (3.45)$$

Eq. (3.45) can be fulfilled by tuning the shape function $S(t)$. If we set $\bar{\epsilon}$ to be the

control before the iteration, $\epsilon^{(0)}$, then Eq. (3.44) becomes

$$\epsilon = \epsilon^{(0)} + 2S(t)\text{Re}\left(\text{Tr}\left[\chi(t)^\dagger \frac{\partial \mathcal{L}^c}{\partial \epsilon} \mathcal{G}\right]\right). \quad (3.46)$$



The new control is obtained by solving Eq. (3.46) and Eq. (3.35), the equation of motion, consistently together with function $\chi(t)$ constructed from Eqs. (3.40) and (3.41).

3.4.2 $F(\mathcal{G}(T))$ second order in state

In Appendix B, we have another definition of fidelity

$$1 - \frac{1}{2N} \text{Tr}\{(O - \mathcal{G}(T))^\dagger (O - \mathcal{G}(T))\} = 1 - \frac{1}{2N} \langle\langle O - \mathcal{G}(T) | O - \mathcal{G}(T) \rangle\rangle.$$

which is second order in $\mathcal{G}(T)$. Define the final time cost $F(\mathcal{G}(T))$ to be $\text{Tr}\{|O - \mathcal{G}(T)|^2\}/2N$, so the minimization of the objective is in accordance with the maximization of the fidelity. A first-order parameter function no longer guarantees the monotonic convergence in the global method since $F(\mathcal{G}(T))$ is not concave with respect to state. We turn to the gradient method introduced in Sec. 3.3.

Note that there is no need for an intermediate cost in this formulation. The parameter function is first order in $\mathcal{G}(t)$

$$\Phi = \langle\langle \chi(t) | \mathcal{G}(t) \rangle\rangle + \langle\langle \mathcal{G}(t) | \chi(t) \rangle\rangle = 2\text{Re}(\text{Tr}[\chi(t)\mathcal{G}(t)]),$$

where $\chi(t)$ satisfies Eqs. (3.29) and (3.30) which in turn are

$$\begin{aligned} |\dot{\chi}\rangle &= (1 \otimes \mathcal{L}^c)^\dagger |\chi\rangle, \\ \chi(T) &= \frac{1}{2N} |O - \mathcal{G}(T)\rangle. \end{aligned}$$

Without the intermediate cost

$$H = \langle \langle \chi | 1 \otimes \mathcal{L}^c | \mathcal{G} \rangle \rangle + \langle \langle \mathcal{G} | (1 \otimes \mathcal{L}^c)^\dagger | \chi \rangle \rangle = 2\text{Re} \left(\text{Tr} \left[\chi^\dagger \mathcal{L}^c \mathcal{G} \right] \right).$$

In Sec. 3.3 we state that $\delta\epsilon$ is determined such that the quantity $\frac{\partial}{\partial\epsilon} R(t, \mathcal{G}^{(0)}, \epsilon^{(0)}) \delta\epsilon$ be positive. We may demand $\delta\epsilon$ to be

$$\delta\epsilon = \frac{\partial}{\partial\epsilon} R(t, \mathcal{G}, \epsilon^{(0)}) = \frac{\partial}{\partial\epsilon} H(t, \chi, \mathcal{G}, \epsilon^{(0)}) = 2\text{Re} \left(\text{Tr} \left[\chi^\dagger \frac{\partial \mathcal{L}^c}{\partial \epsilon} \Big|_{\epsilon^{(0)}} \mathcal{G} \right] \right),$$

so for $w^{(1)}$ close enough to $w^{(0)}$, $\frac{\partial}{\partial\epsilon} R(t, \mathcal{G}^{(0)}, \epsilon^{(0)})$ and $\delta\epsilon$ have the same sign.

The control update rule is then

$$\epsilon = \epsilon^{(0)} + 2\lambda \text{Re} \left(\text{Tr} \left[\chi^\dagger \frac{\partial \mathcal{L}^c}{\partial \epsilon} \Big|_{\epsilon^{(0)}} \mathcal{G} \right] \right), \quad (3.47)$$

where λ is chosen small enough such that the objective is improved. Solving Eq. (47) self-consistently with the equation of motion yields the new process $w^{(1)}$.

3.5 Remarks

In this chapter two kinds of optimization formulation and algorithm are introduced. The global improvement method has the advantage of producing macrosteps in the functional values at every iteration, so it reduces dramatically the necessary amount of calculation compared to the gradient method when the initial process $w^{(0)}$ is far from the local optimal process. However, the formulation of the global improvement method is more complicated and a second-order parameter function is, in general, required. Both methods ensures only the finding of a local optimal process, so it is necessary to carry out the improving iterations with various initial guesses.

On applying optimal control theory to the open quantum systems, two definition of final-time cost (fidelity) are studied. Apart from some subtle difference, the resulting

update rules, Eqs. (3.46) and (3.47), look almost identical. Though, the concept and formulation behind these two equations is quite different.





Chapter 4

Optimal Control of Quantum Gates in Open Systems

4.1 Overview

Combining the exact master equation derived in Chapter 2 and the optimal control theory described in Chapter 3, we are ready to construct the single-qubit quantum gates in open quantum systems using the optimal control theory. In quantum computation, an arbitrary single qubit gate can be built with successive operations of z-rotation and x-rotation. For multi-qubit gates, CNOT-gates and single-qubit gates are considered to be universal. That is, any multiple qubit gate can be obtained as a composition of CNOT-gates and single-qubit gates [25].

In our work we focus on optimal controlling identity gates and z-gates. Identity gate is not a logic gate employed in quantum computation but rather serves as a quantum memory which stores the quantum state in a noisy environment for a certain period of time. Its fidelity characterizes how good a qubit state is able to survive under the influence of the environment.

We start with the dissipative system mentioned in Chapter 2 and with the exponen-

tial decaying correlation function (Lorentzian-like spectral density). Systems with non exponential decaying correlation functions are also considered. Here an environment with an Ohmic spectral density is treated.



4.2 Method

4.2.1 Control problem

In our model, the transition frequency of the two-level system is assumed to be tunable and is treated as the control parameter,

$$\omega_0 \rightarrow \omega_0 + \epsilon(t) \equiv \omega_0(t). \quad (4.1)$$

The master equation of a two level dissipative system with a time dependent transition frequency can be derived following the derivation introduced in Chapter 2. All we have to do is to substitute $\omega_0(t)$ for ω_0 in (2.46)

$$\rho_t = \begin{pmatrix} \rho_{11}(0) \exp\left(-\int_0^t [F(s) + F^*(s)] ds\right) & \rho_{12}(0) \exp\left(-i \int_0^t \omega_0(s) ds - \int_0^t F(s) ds\right) \\ \rho_{21}(0) \exp\left(i \int_0^t \omega_0(s) ds - \int_0^t F^*(s) ds\right) & 1 - \rho_{11}(0) \exp\left(-\int_0^t [F(s) + F^*(s)] ds\right) \end{pmatrix}, \quad (4.2)$$

$$\dot{\rho}_t = \begin{pmatrix} -(F(t) + F^*(t)) \rho_{11}(t) & (-i\omega_0(t) - F(t)) \rho_{12}(t) \\ (i\omega_0(t) - F^*(t)) \rho_{21}(t) & (F(t) + F^*(t)) \rho_{11}(t) \end{pmatrix}, \quad (4.3)$$

where $F(t) \equiv \int_0^t dsc(t, s) f(t, s)$ as in Chapter 2.

Using the vec operation introduced in the last chapter, the above equation becomes

$$\dot{\rho}_t^c = \begin{pmatrix} -(F(t) + F^*(t)) & 0 & 0 & 0 \\ 0 & (i\omega_0(t) - F^*(t)) & 0 & 0 \\ 0 & 0 & (-i\omega_0(t) - F(t)) & 0 \\ F(t) + F^*(t) & 0 & 0 & 0 \end{pmatrix} \rho_t^c \equiv \mathcal{L}(t, \epsilon) \rho_t^c \quad (4.4)$$

If we write

$$\rho_t^c = \mathcal{G}(t)\rho_0^c, \quad (4.5)$$

where $\mathcal{G}(t)$ is the propagator. Then we get the equation of motion for $\mathcal{G}(t)$

$$\begin{cases} \frac{d}{dt}\mathcal{G}(t) = \mathcal{L}(t, \epsilon)\mathcal{G}(t), \\ \mathcal{G}(0) = I. \end{cases} \quad (4.6)$$

From Eq. (4.5) we see that the effect of the propagator can be viewed as a gate operation.

4.2.2 Target

An arbitrary state operated by a z-gate is equivalent to a state vector operated by a Pauli-z matrix,

$$\sigma_z |\psi\rangle = \begin{pmatrix} 1 & 0 \\ 0 & -1 \end{pmatrix} |\psi\rangle. \quad (4.7)$$

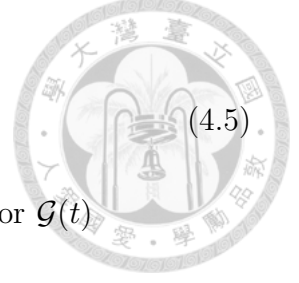
In density matrix form,

$$\sigma_z |\psi\rangle \langle \psi| \sigma_z \rightarrow \sigma_z |\psi\rangle \langle \psi| \sigma_z = \sigma_z \rho \sigma_z. \quad (4.8)$$

Put the above expression in column form:

$$\text{vec}(\sigma_z \rho \sigma_z) = (\sigma_z^T \otimes \sigma_z) \rho^c = \begin{pmatrix} 1 & 0 & 0 & 0 \\ 0 & -1 & 0 & 0 \\ 0 & 0 & -1 & 0 \\ 0 & 0 & 0 & 1 \end{pmatrix} \rho^c. \quad (4.9)$$

So the matrix with diagonal elements (1,-1,-1,1) and otherwise zero is the target for Z-gate control. Denote this target matrix by O_Z , the optimal control theory is applied such that the difference between $\mathcal{G}(t)$ and O_Z is as small as possible.



Similarly, for identity gate, we define

$$O_I = \begin{pmatrix} 1 & 0 & 0 & 0 \\ 0 & 1 & 0 & 0 \\ 0 & 0 & 1 & 0 \\ 0 & 0 & 0 & 1 \end{pmatrix}, \quad (4.10)$$



or the $\pi/8$ -gate

$$O_{\frac{\pi}{8}} = \begin{pmatrix} 1 & 0 & 0 & 0 \\ 0 & e^{i\frac{\pi}{4}} & 0 & 0 \\ 0 & 0 & e^{-i\frac{\pi}{4}} & 0 \\ 0 & 0 & 0 & 1 \end{pmatrix}. \quad (4.11)$$

4.2.3 Gate error and control update

The following definition of gate error is adopted:

$$\frac{1}{2N} \text{Tr} \left\{ (O - \mathcal{G}(t_f))^\dagger (O - \mathcal{G}(t_f)) \right\}, \quad (4.12)$$

where t_f is the final operation time. This error also serve as the objective which we wish to minimize in the optimal control theory. For this objective, a gradient-type optimization algorithm is applied, the control update rule being solving the following two equations simultaneously,

$$\begin{cases} \epsilon = \epsilon^{(0)} + 2\lambda \text{Re} \left(\text{Tr} \left[\chi^\dagger \frac{\partial \mathcal{L}}{\partial \epsilon} \Big|_{\epsilon^{(0)}} \mathcal{G} \right] \right), \\ \frac{d}{dt} \mathcal{G}(t) = \mathcal{L}(t, \epsilon) \mathcal{G}(t). \end{cases} \quad (4.13)$$

Here $\chi(t)$ is the adjoint function defined in Chapter 3.



4.2.4 Range of control parameter

Practically, the control parameter - in our case the transition frequency - must be constrained in a certain range. An overwhelmingly large magnitude of control may yield a good performance in a short time but may well be impossible to realize experimentally. Sometimes the original system is destroyed well before the desired control strength is reached. In our work, we constrain the control to range form $|\epsilon(t)| \leq \omega_0$, where ω_0 is the original system frequency.

The simplest way is to set a range and manually “chop off” the control when it exceeds the limit. Another way is to define the control parameter as a trigonometric function of some angle $\theta(t)$

$$\epsilon(t) \equiv A \sin(\theta(t)), \quad (4.14)$$

and the update equation becomes

$$\begin{aligned} \theta^{(1)} &= \theta^{(0)} + \frac{1}{S(t)} \operatorname{Re} \left\{ \operatorname{Tr} \left[\chi^{(0)}(t) \frac{\partial \mathcal{L}}{\partial \theta} \Big|_{\theta^{(0)}} \mathcal{G}^{(1)}(t) \right] \right\} \\ &= \theta^{(0)} + \frac{A \cos(\theta^{(0)}(t))}{S(t)} \operatorname{Re} \left\{ \operatorname{Tr} \left[\chi^{(0)}(t) \frac{\partial \mathcal{L}}{\partial \theta} \Big|_{\theta^{(0)}} \mathcal{G}^{(1)}(t) \right] \right\}, \end{aligned} \quad (4.15)$$

and

$$\epsilon^{(1)}(t) = A \sin(\theta^{(k+1)}(t)). \quad (4.16)$$

Thus the control is constrained in the desired range $|\epsilon| \leq A$ due to its functional nature. A drawback of this setup is that the control parameter cannot update when the initial guess is set right at the upper/lower limit, i.e., when $\cos(\theta^{(0)}) = 0$. So we use these two methods interchangeably.



4.2.5 Initial guess

In the ideal case where there is no environment effect (closed system), identity gates and Z-gates are easily achieved by rotation due to the system Hamiltonian proportional to σ_z . In this case the propagator is

$$\mathcal{G}(t) = \begin{pmatrix} 1 & 0 & 0 & 0 \\ 0 & e^{i \int_0^t \omega_0(s) ds} & 0 & 0 \\ 0 & 0 & e^{-i \int_0^t \omega_0(s) ds} & 0 \\ 0 & 0 & 0 & 1 \end{pmatrix}.$$

To build a identity gate, we demand $\int_0^t \omega_0(s) ds = n\pi$, where $n = 0, 2, 4, \dots$. A Z-gate requires $\int_0^t \omega_0(s) ds = m\pi$, where $m = 1, 3, 5, \dots$. In the case where the final time t_f is fixed, a naive design of control could be

$$\omega_0(t) = \omega_0 + \epsilon(t) = \frac{p \cdot \pi}{t_f} \quad (4.17)$$

where $p = n$ for identity gates and $p = m$ for Z-gates. The control constructed this way is a square-wave pulse whose duration is t_f (initial time $t_0 = 0$). In open systems, if the environment effect is not too overwhelming, the ideal closed system control pulse is a good starting point for the optimization iteration and is taken as the initial guess. Note that p should be chosen such that $\epsilon(t) < A$. In the following, $A = \omega_0$ if not stated otherwise.

4.3 Results

In this section we present some results of constructing quantum gates using optimal control. All the parameters are in units of the system transition frequency ω_0 if not stated explicitly.

4.3.1 Lorentzian-like spectral density

The Lorentzian spectral density,

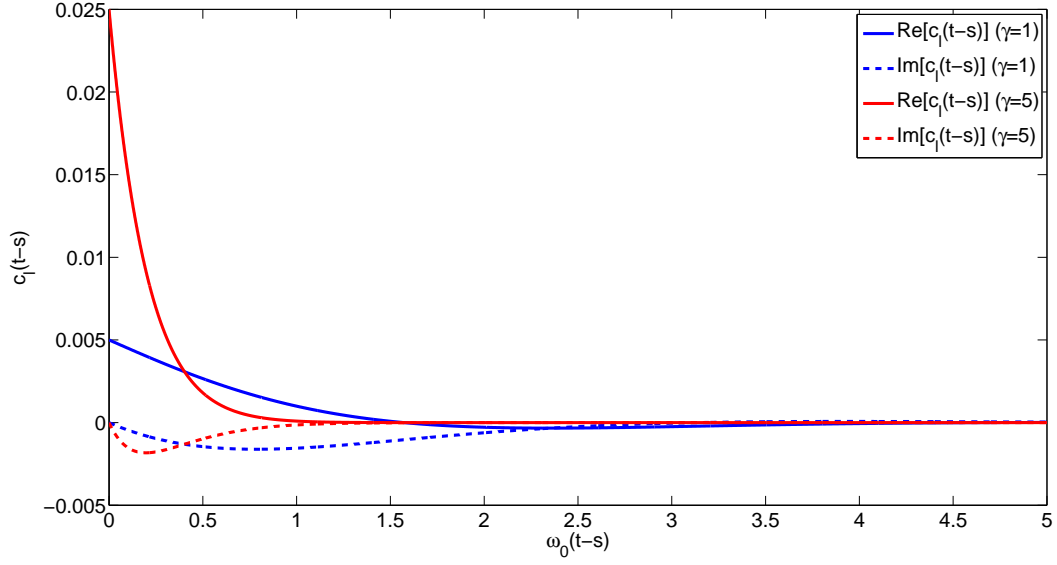
$$D_l(\omega) = \frac{\alpha}{2\pi} \frac{\gamma^2}{(\omega - \Omega)^2 + \gamma^2}, \quad (4.18)$$

yields the exponential decaying bath correlation function,

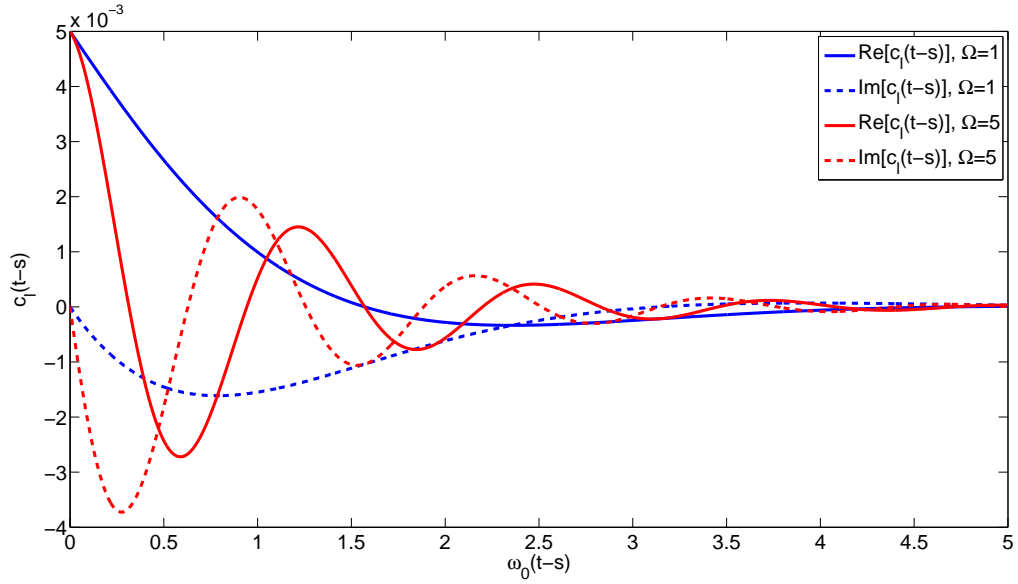
$$c_l(t-s) = \int_0^\infty d\omega D_l(\omega) e^{-i\omega(t-s)} \approx \alpha \frac{\gamma}{2} \exp[-\gamma|t-s| - i\Omega(t-s)], \quad (4.19)$$

when the central frequency of the environment spectrum Ω is substantially larger than the Lorentzian width γ (Appendix A). In the following we consider the bath correlation function in the form of Eq. (4.19) which corresponds to a “Lorentzian-like” spectral density and disregard the condition where the approximation in Eq. (4.19) is valid. The relevant parameters are the correlation strength α , the correlation time γ^{-1} , and the central frequency of the environment spectrum Ω . Figure 4.1 shows the correlation function under various conditions.





(a) Correlation function at $\Omega = 1$ for various values of γ .



(b) Correlation function at $\gamma = 1$ for various values of Ω .

Figure 4.1: Lorentzian-like correlation function plotted at various conditions. Here $\alpha = 0.01$.

4.3.2 Identity gate

Figure 4.2 shows the gate error of identity gate control vs. operation time. High fidelity gates with error $\lesssim 10^{-4}$ can be achieved for operation time longer than the

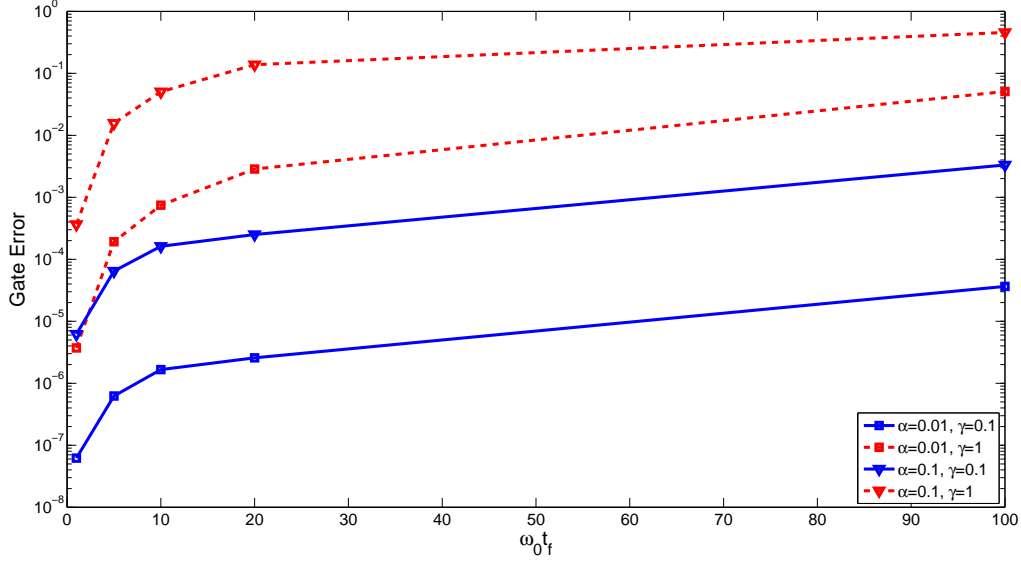


Figure 4.2: Gate error of identity-gate control vs. operation time. Here the environment central frequency coincides with the system transition frequency, *i.e.*, $\Omega = \omega_0$.

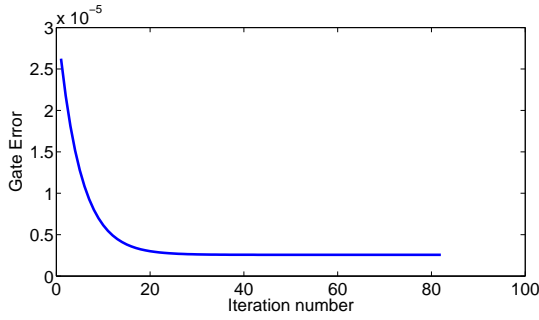
system decay time for moderate system decay parameters. The gate control is better performed with weaker system-environment coupling strength (α small) and with larger correlation time (γ small).

Figure 4.3 shows plots of gate error vs. iteration number and a typical control pulse. Note that the error vs. iteration profile demonstrates the monotonic converging behavior of the optimization iteration. It also shows saturation of the error near an optimal trajectory.

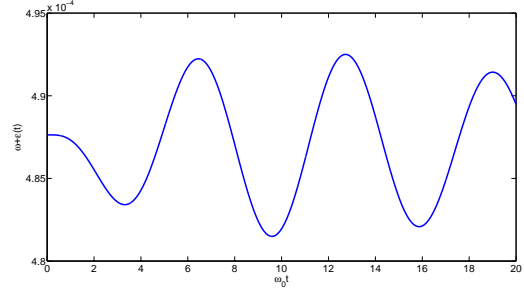
4.3.3 Improvement

An important question to be addressed is that, how much can the optimal control algorithm improve the gate fidelity in an open quantum system, given that we take the ideal closed system control pulse as our initial guess. Define the improvement to be

$$Imp \equiv \lim_{n \rightarrow \infty} \frac{Er^{(0)}}{Er^{(n)}}, \quad (4.20)$$



(a) Gate error vs. iteration number.



(b) A typical control pulse for identity gate control, plotted at $\alpha = 0.01$, $\gamma = 0.1$, and $t_f = 20$.

Figure 4.3: The gate error vs. iteration profile and a typical control pulse for identity gate control.

where $Er^{(0)}$ denotes the gate error before the optimization iteration when the ideal closed system control pulse is taken as the initial guess, and $Er^{(n)}$ is the gate error after n rounds of optimization iteration. The improvement Imp corresponds to the possibility of improving the gate error in an open quantum system by the optimal control theory. A large improvement indicates that optimal control theory is useful and powerful in correcting the error caused by the environment effect. A small improvement, however, shows that optimal control does not play an important role for the open system and an ideal closed system optimal control pulse suffices.

Figure 4.4 shows the improvement vs. the operation time under various conditions. It is obvious that for environment effects with a long correlation time ($\gamma = 0.1$), the improvement can be up to an order. However, short time environment effects ($\gamma = 1$) can hardly be corrected. Also note that the improvement increases as the operation time gets longer, this is due to the fact that the longer the operation time is, the better that optimal control can come into play and correct the error. The overall coupling strength α does not play a role in the improvement.

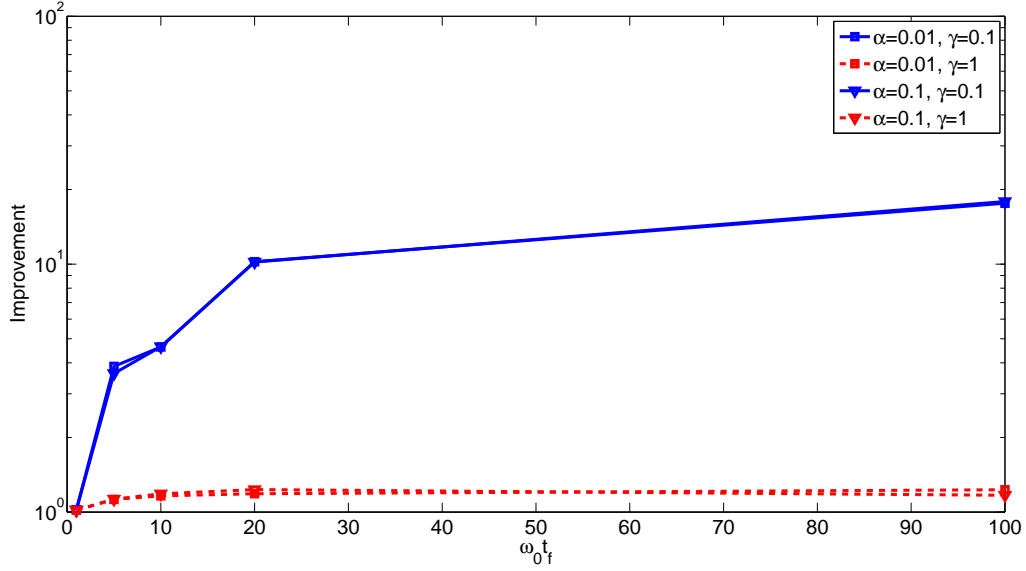


Figure 4.4: Improvement vs. operation time with $\Omega = \omega_0$ for various conditions.

4.3.4 Z-gate

In contrast to the identity-gate control where we wish the qubit state to maintain in its initial state as long as possible, in Z-gate control we desire the operation to be fast. Recall that the ideal closed-system pulse, which is our initial guess, and final time should comply with Eq. (4.17). We choose the final time t_f to be the shortest integer of ω_0^{-1} where a π rotation can be completed within the admissible control range. That is, $t_f = 2/\omega_0$ and $\epsilon(t) = \pi/2 - 1$. The results are shown in Table 4.1. Figure 4.5 gives the error vs. iteration profile and a typical control pulse shape.

$\alpha \backslash \gamma$	0.1	1	10
0.01	$9.15 \times 10^{-7} \rightarrow 8.89 \times 10^{-7}$	$3.68 \times 10^{-5} \rightarrow 3.53 \times 10^{-5}$	$1.10 \times 10^{-4} \rightarrow 1.10 \times 10^{-4}$
0.1	$9.10 \times 10^{-5} \rightarrow 8.81 \times 10^{-5}$	$3.36 \times 10^{-3} \rightarrow 3.31 \times 10^{-3}$	$9.57 \times 10^{-3} \rightarrow 9.57 \times 10^{-3}$
1	$8.22 \times 10^{-3} \rightarrow 8.06 \times 10^{-3}$	$1.79 \times 10^{-1} \rightarrow 1.78 \times 10^{-1}$	$2.86 \times 10^{-1} \rightarrow 2.86 \times 10^{-1}$

(a) $\Omega = \omega_0$

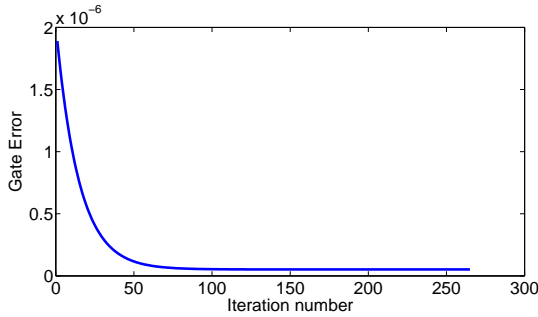
$\alpha \backslash \gamma$	0.1	1	10
0.01	$1.89 \times 10^{-8} \rightarrow 5.17 \times 10^{-10}$	$2.93 \times 10^{-6} \rightarrow 1.40 \times 10^{-6}$	$9.29 \times 10^{-5} \rightarrow 9.15 \times 10^{-5}$
0.1	$1.89 \times 10^{-6} \rightarrow 5.18 \times 10^{-8}$	$2.86 \times 10^{-4} \rightarrow 1.37 \times 10^{-4}$	$8.15 \times 10^{-3} \rightarrow 7.98 \times 10^{-3}$
1	$1.86 \times 10^{-4} \rightarrow 5.35 \times 10^{-6}$	$2.31 \times 10^{-2} \rightarrow 1.10 \times 10^{-2}$	$2.67 \times 10^{-1} \rightarrow 2.59 \times 10^{-1}$

(b) $\Omega = 5\omega_0$

$\alpha \backslash \gamma$	0.1	1	10
0.01	$4.00 \times 10^{-9} \rightarrow 1.54 \times 10^{-10}$	$3.94 \times 10^{-7} \rightarrow 5.63 \times 10^{-8}$	$4.69 \times 10^{-5} \rightarrow 4.16 \times 10^{-5}$
0.1	$4.00 \times 10^{-7} \rightarrow 1.54 \times 10^{-8}$	$3.92 \times 10^{-5} \rightarrow 5.60 \times 10^{-6}$	$4.29 \times 10^{-3} \rightarrow 3.79 \times 10^{-3}$
1	$4.02 \times 10^{-5} \rightarrow 1.57 \times 10^{-6}$	$3.78 \times 10^{-3} \rightarrow 5.31 \times 10^{-4}$	$1.95 \times 10^{-1} \rightarrow 1.67 \times 10^{-1}$

(c) $\Omega = 10\omega_0$

Table 4.1: Z-gate error under various conditions with a Lorentzian-like spectral density. The value before the arrow denotes the error generated from the ideal closed system control pulse and the value after the arrow denotes the saturate error after the optimization iterations.



(a) Gate error vs. iteration number.

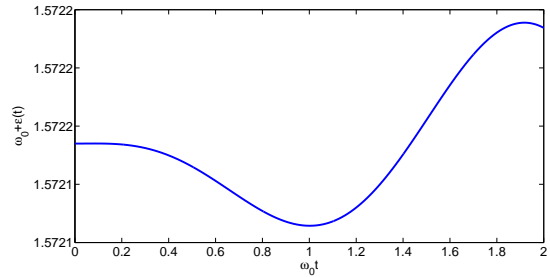
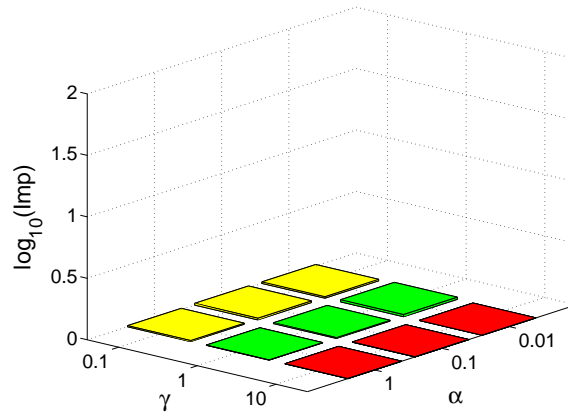
(b) A typical control pulse for z-gate control, plotted at $\alpha = 0.1$, $\gamma = 0.1$, and $\Omega = 5$.

Figure 4.5: (a) Gate error vs. iteration profile and (b) a typical control pulse for Z-gate control.

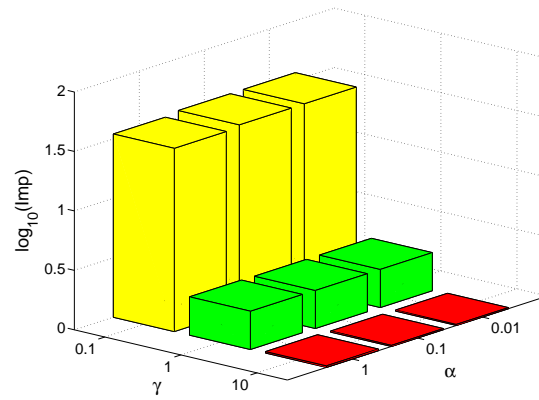
The results show similar trends with the identity gate control that the Z-gate control is better performed and has a smaller gate error when the environment effect is

weak in the overall strength (α small) or relatively non-Markovian (γ small). The Z-gate operation time is short compared to the identity gate operation time, so the improvement defined in Eq. (4.20) is small in the case where $\Omega = \omega_0$. However, we found that the improvement increases considerably if we set $\Omega = 5\omega_0$ or $\Omega = 10\omega_0$.

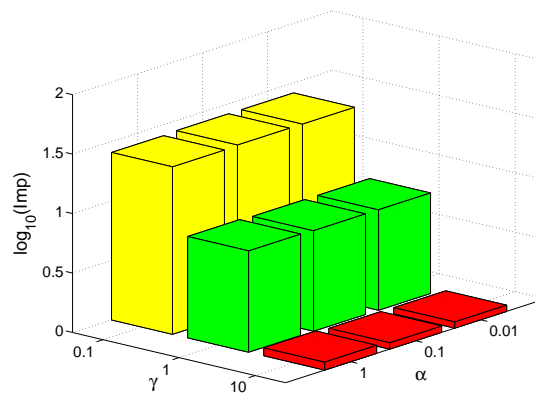
Figure 4.6 shows the plot of the improvement of the Z-gate control under various conditions. Apparently there is hardly any improvement when Ω is equal to the system transition frequency. As the detuning ($\Omega - \omega_0$) grows large, we observe great improvement in the Z-gate control up to one to two order of magnitude. The increase in the improvement is not monotonic. Note that in Fig. 4.6(b) and 4.6(c) the improvement at $\gamma = 0.1$ and $\Omega = 10\omega_0$ is less than that at $\gamma = 0.1$ and $\Omega = 5\omega_0$. Improvement is also larger when the bath correlation time (γ^{-1}) is longer. The parameter α does not play a role in the improvement.



(a) Plotted at $\Omega = \omega_0$.



(b) Plotted at $\Omega = 5\omega_0$.



(c) Plotted at $\Omega = 10\omega_0$.

Figure 4.6: Improvement of Z-gate control in a Lorentzian-like environment under various conditions. Here the values of α and γ are in units of ω_0 .

4.4 Ohmic spectral density



In this section, we adopt the spectral density which is commonly used in modeling the environment. The bosonic spectral density may be parametrized as

$$D_o(\omega) = 2\alpha_o\omega_c^{1-x}\omega^x e^{-\omega/\omega_c}. \quad (4.21)$$

Here α_o is a dimensionless coupling parameter (similar to the parameter α in the Lorentzian-like spectral density but is dimensionless) and ω_c is the cutoff frequency. The parameter x determines the low-frequency behavior of $D_o(\omega)$. Couplings with

- $x < 1$: sub-ohmic
- $x = 1$: ohmic
- $x > 1$: super-ohmic

This classification has its origin in the analysis of the dissipative two-level system [26]. The correlation function is then expressed analytically as

$$c_o(t-s) \equiv \int_0^\infty D_o(\omega) e^{-i\omega(t-s)} = 2\alpha_o\omega_c^{x+1}\Gamma(x+1)(1+i\omega_c(t-s))^{-(x+1)}, \quad (4.22)$$

where $\Gamma(x)$ is the gamma function and $\Gamma(x) = (x-1)!$ when x is a positive integer. In the following we focus on the Ohmic spectral density where $x = 1$ and vary the cutoff ω_c and coupling α_o .

Figure 4.7 shows the corresponding correlation function. Note that this correlation function is no longer exponential in time and a function fitting is needed.

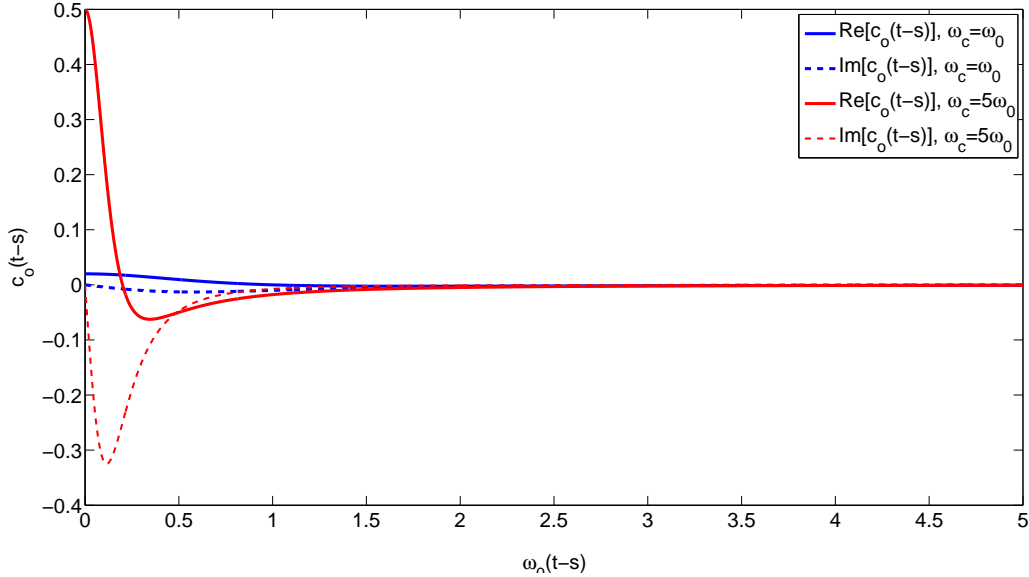
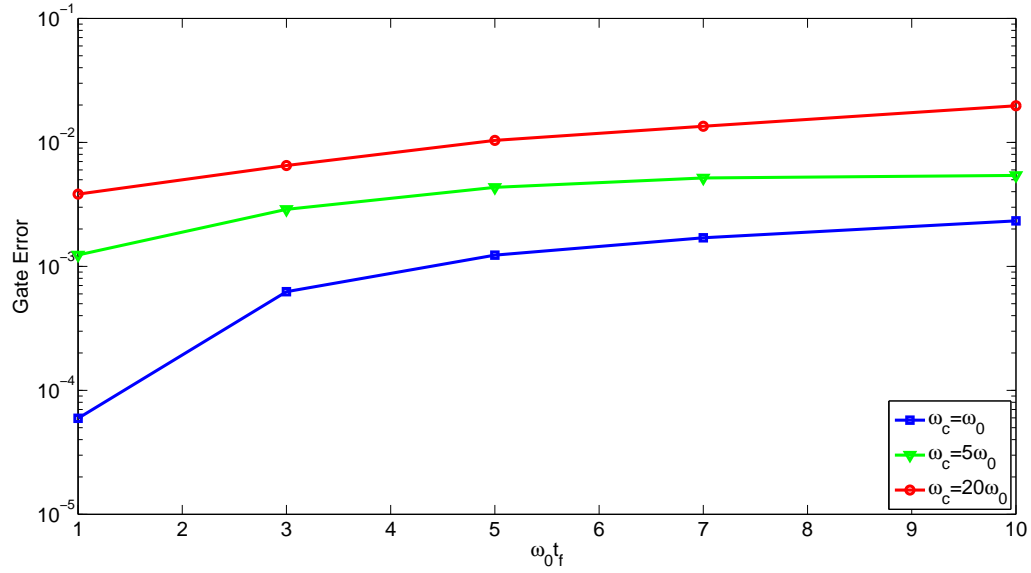


Figure 4.7: Correlation function corresponding to an Ohmic spectral density with $\alpha_o = 0.01$ for various cutoff frequencies.

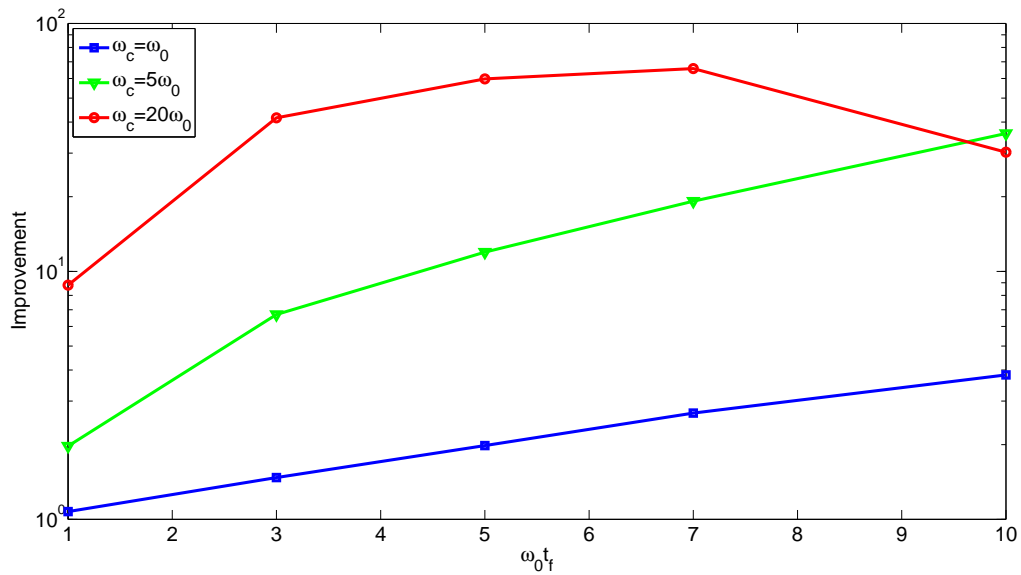
4.4.1 Identity gate

Figure 4.8 shows the gate error and improvement vs. operation time for various cutoff frequencies. The gate control is performed with smaller cutoff frequencies and shorter operation time. The relation between the gate error and the cutoff frequency could be understood by inspecting the plot for the correlation function, Fig. 4.7. When the environment spectral density has a higher cutoff frequency, the correlation time of system-environment is shorter, and the environment effect becomes stronger in weight at the beginning of the operation time. This is similar to the effect of small γ^{-1} in the Lorentzian-like case.

The improvement also increases along with the cutoff frequency and with the operation time. Unlike the Lorentzian-like case, where improvement is large when the environment effect is relatively non-Markovian (γ small), in an Ohmic environment, large improvement corresponds to cases where the environment effect is more Markovian (ω_c large). We shall study this behavior further in the following sections.



(a) Gate error vs. operation time.



(b) Improvement vs. operation time.

Figure 4.8: Plots of identity gate control for various cutoff frequencies, $\alpha_o = 0.01$.

$\alpha \backslash \omega_c$	1	5	20
10^{-4}	$9.74 \times 10^{-8} \rightarrow 9.73 \times 10^{-8}$	$2.76 \times 10^{-6} \rightarrow 1.97 \times 10^{-6}$	$2.29 \times 10^{-5} \rightarrow 4.64 \times 10^{-6}$
10^{-3}	$9.71 \times 10^{-6} \rightarrow 9.70 \times 10^{-6}$	$2.71 \times 10^{-4} \rightarrow 1.93 \times 10^{-4}$	$2.23 \times 10^{-3} \rightarrow 4.52 \times 10^{-4}$
10^{-2}	$9.40 \times 10^{-4} \rightarrow 9.40 \times 10^{-4}$	$2.23 \times 10^{-2} \rightarrow 1.58 \times 10^{-2}$	$1.66 \times 10^{-1} \rightarrow 3.22 \times 10^{-2}$

Table 4.2: Z-gate error under various conditions with an Ohmic spectral density. The value before the arrow denotes the error generated from the ideal closed system control pulse and the value after the arrow denotes the saturate error after the optimization iterations.

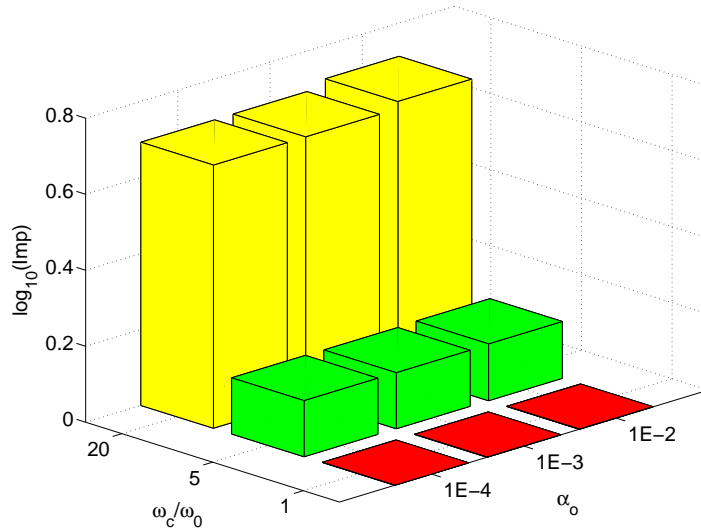


Figure 4.9: Improvement of Z-gate control in a Ohmic environment under various conditions with the Ohmic spectral density.

4.4.2 Z-gate

Table 4.2 shows the errors of the initial closed system pulse and errors after the optimal control iterations. Figure 4.9 shows the improvement under various conditions.

Similar to the Lorentzian-like case, α_o does not play an important role in improvement. Improvement increases with the cutoff frequency as in the identity gate control in the previous section. We discuss this somewhat anomalous trend in the next section.

4.5 Environment suppression ability of optimal control



4.5.1 Error correction due to phase shift

Recall that in our model the exact solution of the density operator can be found. In Eq. (4.2),

$$\rho_t = \begin{pmatrix} \rho_{11}(0) \exp\left(-\int_0^t [F(s) + F^*(s)] ds\right) & \rho_{12}(0) \exp\left(-i \int_0^t \omega_0(s) ds - \int_0^t F(s) ds\right) \\ \rho_{21}(0) \exp\left(i \int_0^t \omega_0(s) ds - \int_0^t F^*(s) ds\right) & 1 - \rho_{11}(0) \exp\left(-\int_0^t [F(s) + F^*(s)] ds\right) \end{pmatrix}. \quad (4.23)$$

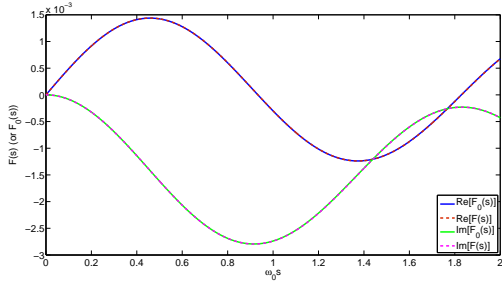
In this form it is clear that the real part of the integration of $F(s)$ encodes the dissipation caused by the environment, and the imaginary part encodes the phase shift of the coherence term resulted from the shift in the system frequency due to the presence of the environment. It is therefore desirable to check how $F(s)$ behaves before and after the optimization iteration.

Upon inspecting several data where notable improvement is observed, it turns out that there exists negligible difference before and after the optimization iteration, in both real and imaginary part of $F(s)$. Fig. (4.10) shows $F(s)$ before and after the optimization improvement.

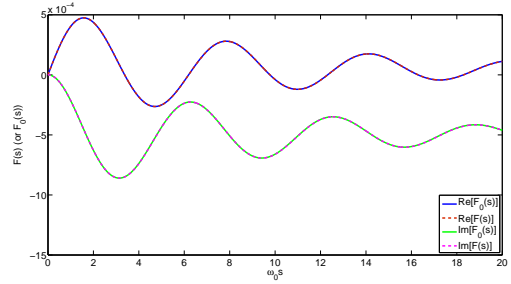
Since we observe little suppression of the dissipation caused by the environment, the only possible agent of correcting the gate error by the optimal control is then through correcting the phase shift. The coherence term (ρ_{21} in particular) in Eq. (4.23) is

$$\begin{aligned} \rho_{21}(t) &= \rho_{21}(0) \exp\left(i \int_0^t \omega_0(s) ds - \int_0^t F^*(s) ds\right) \\ &= \rho_{21}(0) \exp\left(-\int_0^t \text{Re}[F(s)] ds\right) \exp\left(i \left(\int_0^t \omega_0(s) ds + \int_0^t \text{Im}[F(s)] ds\right)\right) \end{aligned} \quad (4.24)$$

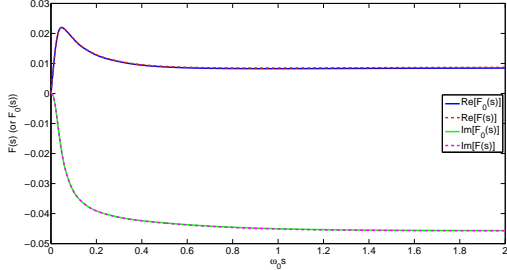
where $\text{Re}[\dots]$ and $\text{Im}[\dots]$ denote the real and imaginary part, respectively. The first



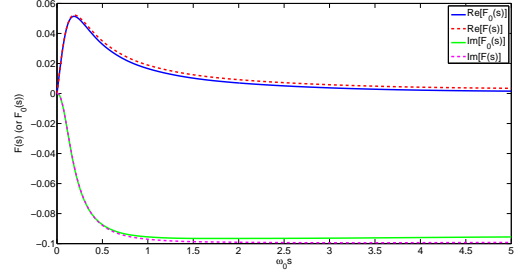
(a) $F(s)$ before and after a Z-gate control in a Lorentzian-like environment. $\alpha = 0.1$, $\gamma = 1$, and $\Omega = 5$. $Imp = 36.56$ in this case.



(b) $F(s)$ before and after an identity gate control in a Lorentzian-like environment. $\alpha = 0.01$, $\gamma = 0.1$, and $\Omega = 1$. $Imp = 10.23$ in this case.



(c) $F(s)$ before and after a Z-gate control in an Ohmic environment. $\alpha_o = 0.001$ and $\omega_c = 20$. $Imp = 4.93$ in this case.



(d) $F(s)$ before and after an identity gate control in an Ohmic environment, plotted at $\alpha_o = 0.01$ and $\omega_c = 5$. $Imp = 11.96$.

Figure 4.10: Comparison of the function $F(s)$ before and after the optimal control. Here $F_0(s)$ denotes the function before the control iteration and $F(s)$ denotes the function after the iteration.

exponential term represents the dissipation effect and the second represents the phase shift. A quick check in the exponent of the phase shift term shows that the phase shift is corrected by the optimal control iteration, as shown in Table 4.3, where the phase difference is defined $(\int_0^{t_f} \omega_0(s) ds + \int_0^{t_f} \text{Im}[F(s)] ds) / \pi$ for the identity gate control and $(\int_0^{t_f} \omega_0(s) ds + \int_0^{t_f} \text{Im}[F(s)] ds) / \pi - 1$ for the Z-gate control.

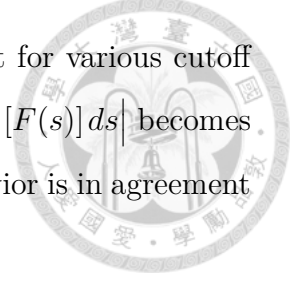
	4a	4b	4c	4d
Phase difference before control	-8.63×10^{-4}	-3.10×10^{-3}	-2.72×10^{-2}	-1.46×10^{-1}
Phase difference after control	-6.66×10^{-8}	-8.11×10^{-7}	-1.59×10^{-4}	-2.18×10^{-3}

Table 4.3: Phase difference of various cases before and after the optimal control iteration.

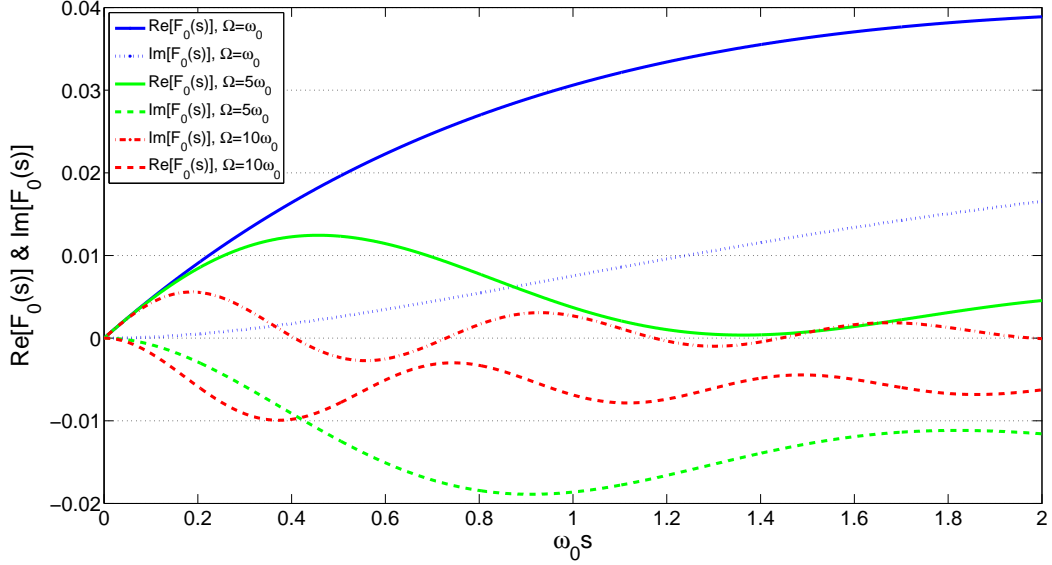
4.5.2 Conditions for mass improvement

We have seen from the previous section that two effects contribute to the gate error, namely the dissipation and the phase shift. The phase shift can be corrected by the optimal control iteration; the dissipation, however, can hardly be suppressed. This indicates that the improvement, *Imp*, is determined by the relative proportion of error that these two effects lead to. For a system where the environment-induced dissipation is the dominant source of gate error, the improvement is limited, since after the optimal control iteration only a minor portion of error can be corrected. On the contrary, if in a system the gate error mainly comes from the environment-induced phase shift, then after the optimal control iteration the improvement can be substantial.

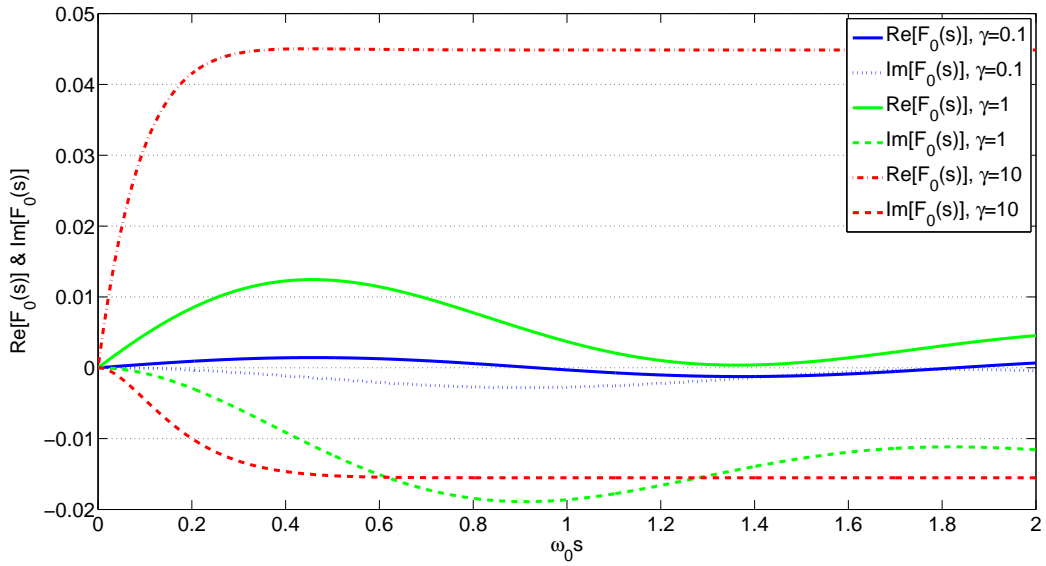
Mathematically, the dissipation and the phase shift are directly related to the magnitude of $|\int_0^{t_f} \text{Re}[F(s)] ds|$ and $|\int_0^{t_f} \text{Im}[F(s)] ds|$. We inspect the plots of $F(s)$ before the optimal control iteration with both the Lorentzian-like environment and Ohmic environment to verify this point. In Fig. 4.11(a), the function $F(s)$ is plotted in an Lorentzian-like environment for various Ω 's and with $\gamma = 1$, and in Fig. 4.11(b), Ω is set at $5\omega_0$ and $F(s)$ is plotted for various γ 's. We can infer that the relative magnitude of $|\int_0^{t_f} \text{Im}[F(s)] ds|$ over $|\int_0^{t_f} \text{Re}[F(s)] ds|$ is larger when Ω is larger or when γ is smaller.



In Fig. 4.12, the function $F(s)$ is plotted in an Ohmic environment for various cutoff frequencies. The relative magnitude of $\left| \int_0^{t_f} \text{Im}[F(s)] ds \right|$ over $\left| \int_0^{t_f} \text{Re}[F(s)] ds \right|$ becomes larger as the cutoff frequency increases. In all of the cases, this behavior is in agreement with a larger improvement.



(a) Function $F_0(s)$ before the optimal control iteration under various Ω 's with $\gamma = 1$.



(b) Function $F_0(s)$ before the optimal control iteration under various γ 's with $\Omega = 5$.

Figure 4.11: The function $F_0(s)$ in an Lorentzian-like environment under various conditions.

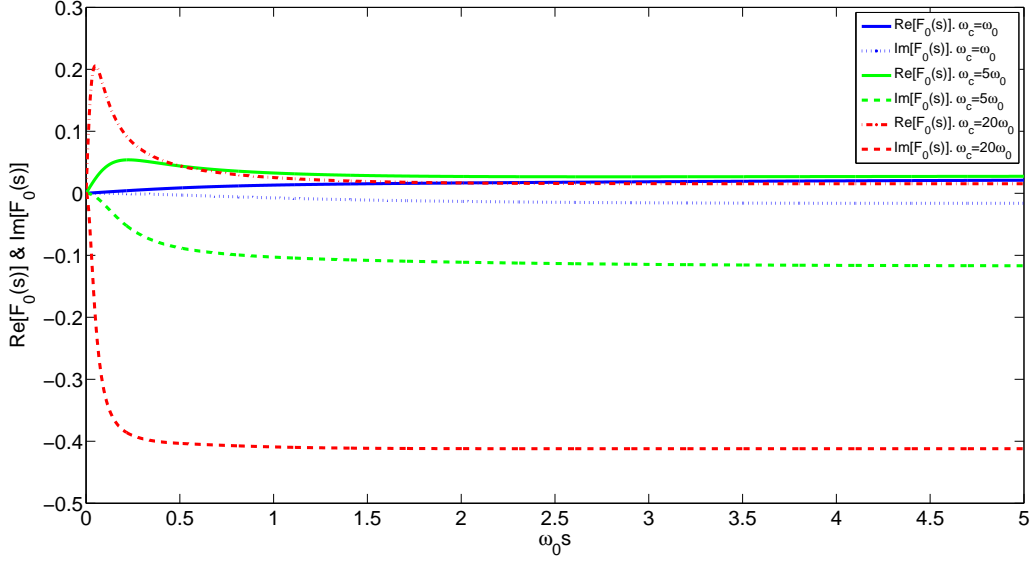


Figure 4.12: $F_0(s)$ in an Ohmic environment at various cutoff frequency.

The behavior of $F(s)$ is determined by its differential equation, Eq. (2.48),

$$\partial_t F_j(t) = p_j + F_j(t) \left[q_j + i\omega_0(t) + \sum_{k \neq j} F_k(t) \right] + F_j^2(t).$$

Mathematically, it is possible to find the conditions that make $\left| \int_0^{t_f} \text{Im}[F(s)] ds \right|$ relatively larger than $\left| \int_0^{t_f} \text{Re}[F(s)] ds \right|$ and thus determine the conditions for mass improvement. To gain some insight on the physics, we may turn to the time-convolutionless perturbative master equation for the two-level dissipative system with a zero-temperature bath [20],

$$\dot{\rho} = -\frac{i}{2}(\omega_0 + \Delta)[\sigma_z, \rho] + \Gamma \left(\sigma_- \rho \sigma_+ - \frac{1}{2} \{ \sigma_+ \sigma_-, \rho \} \right), \quad (4.25)$$

where

$$\Delta \equiv P \int_0^\infty d\omega \frac{D(\omega)}{\omega_0 - \omega} \quad (4.26)$$

is the environment-induced frequency shift (Lamb shift) and is defined as the Cauchy's principle value P of a improper integral over the spectral density with a weighting $(\omega_0 - \omega)^{-1}$. Note that the weighting is positive when $\omega_0 > \omega$ and negative when $\omega_0 < \omega$.

The decay rate Γ is defined as the value of the spectral density at the qubit transition frequency,

$$\Gamma \equiv 2\pi D(\omega_0). \quad (4.27)$$

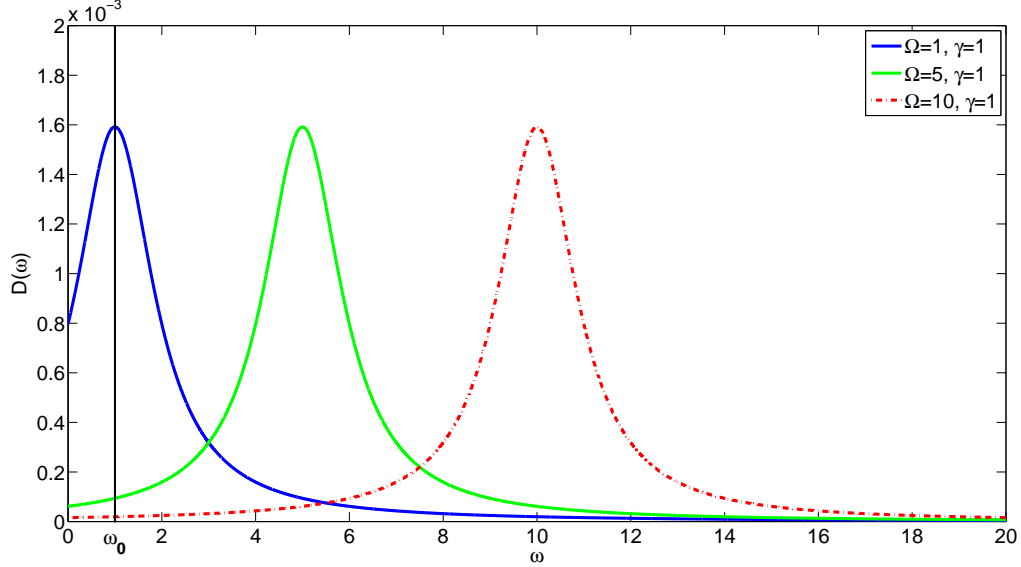
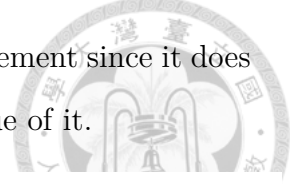
The Lamb shift and the decay rate in general depend on time and this time-convolutionless perturbative master equation is valid only in weak interaction regime and when the system-environment correlation time is much shorter than the operation time. Nevertheless, Equation (4.25) is in complete analogy to the exact master equation, Eq. (2.46), and the real part and the imaginary part of $F(t)$ can be mapped to the constants Γ and Δ . By definition, Γ and Δ are determined completely by the environment spectral density $D(\omega)$ and are in close relation to the shape of it.

Figure 4.13(a) shows the spectral density and the relative position of the qubit transition frequency ω_0 . For the case of zero-detuning, $\Omega = \omega_0$, the spectral density is symmetric with respect to ω_0 . The decay rate $\Gamma \equiv 2\pi D(\omega_0)$ turns out to be at the peak value of the Lorentzian distribution, while the Lamb shift Δ defined in Eq. (4.26) becomes vanishingly small due to mutual cancellation in the integration. In this situation the dissipation effect dominates over the phase shift effect, and the improvement due to the optimal control is limited. However, if the environment central frequency is detuned from the qubit's transition frequency, the decay rate defined in Eq. (4.27) drops dramatically, and the Lamb shift defined in Eq. (4.26) increases due to the asymmetric distribution of the spectral density with respect to ω_0 . This is in agreement with the trend of improvement observed in the previous sections. Note that this behavior is more prominent as the Lorentzian distribution gets sharper (γ small).

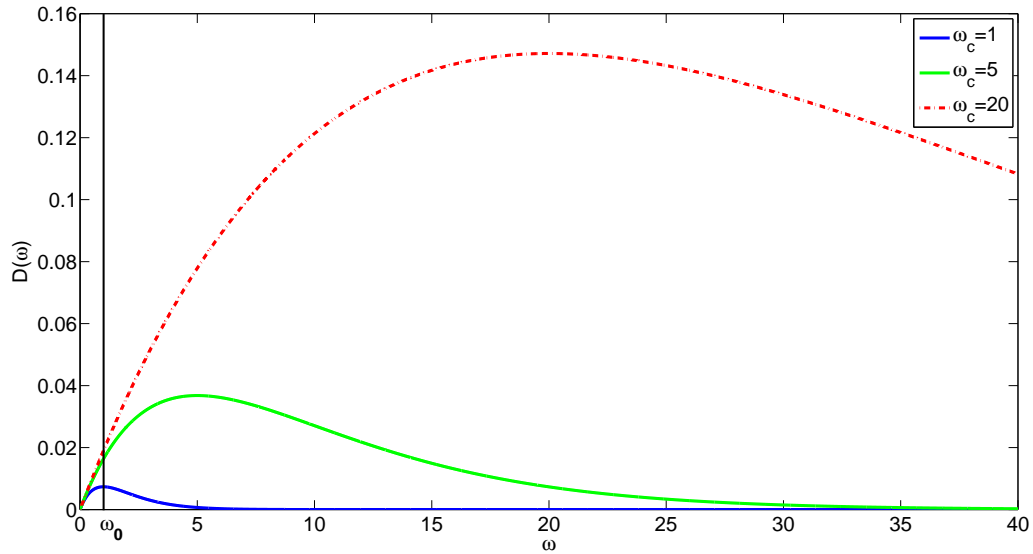
In Fig. 4.13(b), a similar plot is demonstrated for the Ohmic spectral density. As the cutoff frequency ω_c increases, the decay rate Γ grows only slightly, whereas the Lamb shift Δ grows substantially due to the asymmetric growth of the spectral density with respect to ω_0 . This behavior leads to the fact that the improvement is larger when the cutoff frequency is increased.



The overall coupling strength α (or α_o) is irrelevant to the improvement since it does not affect the shape of the spectral density but only the overall value of it.



(a) The Lorentzian spectral density plotted under various environment central frequencies. Here $\alpha = 0.01$.



(b) The Ohmic spectral density plotted under various cutoff frequencies with $\alpha_o = 0.01$.

Figure 4.13: The spectral density of a Lorentzian environment and an Ohmic environment. The relative position of the qubit transition frequency ω_0 is shown.

Although the above qualitative argument is applied to a time-convolutionless perturbative master equation and not to the exact dynamics, it shows the important fact

that, the shape of the spectral density is in close relation to the improvement. The shape of the spectral density determines the decay rate and the Lamb shift, which in turn determines the magnitude of the improvement. The improvement is maximized when the system suffers from a small decay rate and a strong Lamb shift.

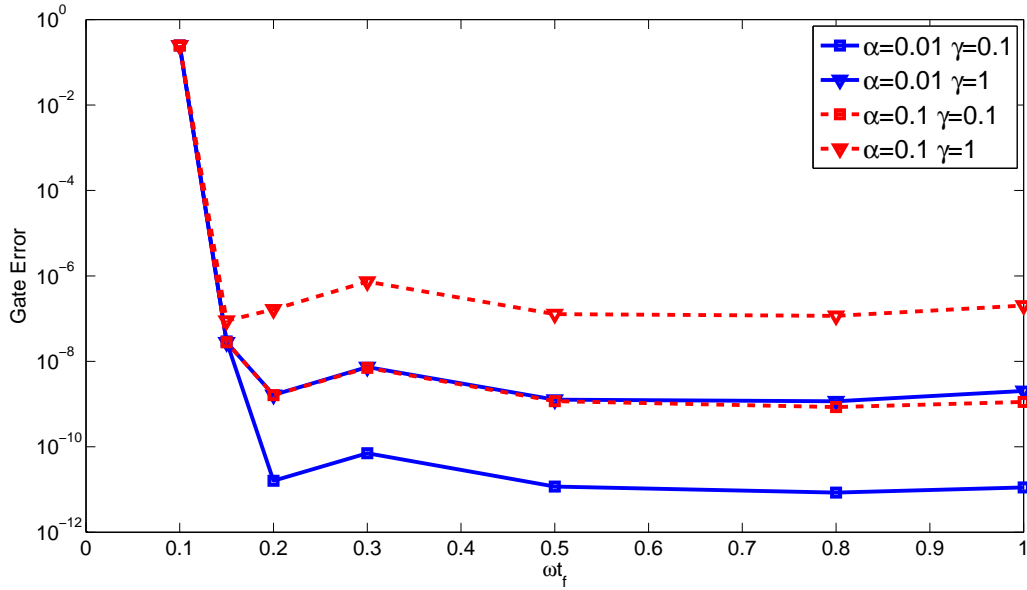
4.5.3 Suppression of dissipation

So far, we have observed very limited effect of suppressing the dissipation using the optimal control iteration for the two-level dissipative model. This behavior is model specific, and is due to the small range of control we choose in the beginning of the control problem. As shown is Eq. (4.24), the control pulse can be designed to directly cancel the environment-induced phase shift, but can hardly suppress the dissipation effect through minimizing the magnitude of $\text{Re} \left[\int_0^{t_f} [F(s)] ds \right]$. A close inspection of the differential equation of $F(t)$ in a Lorentzian-like spectral density, Eq. (2.50),

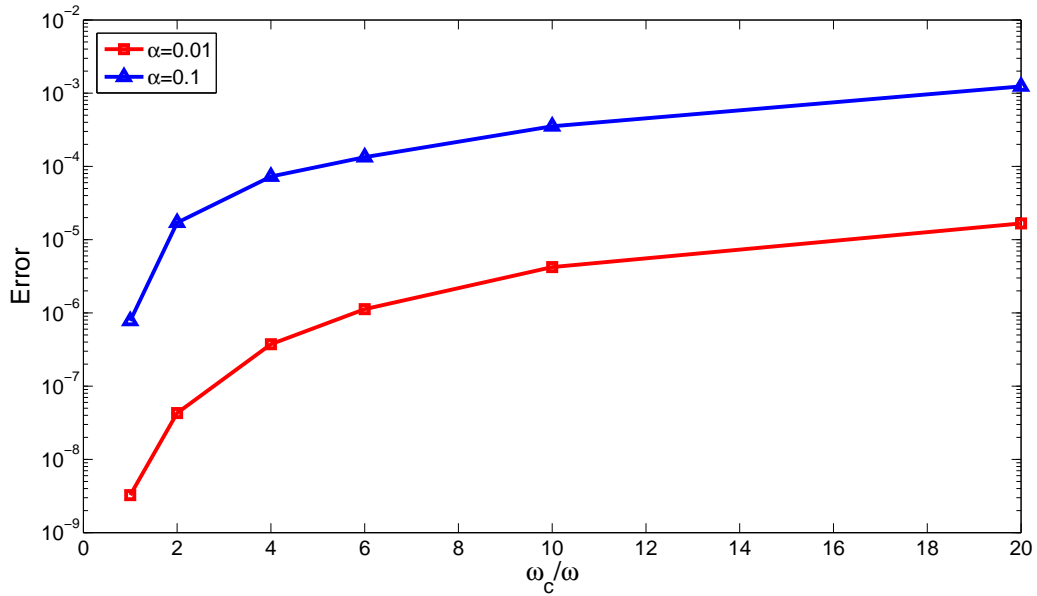
$$\partial_t F(t) = -\gamma F(t) + i(\omega_0 - \Omega + \epsilon(t)) F(t) + F(t)^2 + \frac{\alpha\gamma}{2},$$

may provide us some idea. In this equation, $\epsilon(t)$ follows the unit imaginary number i , so $F(t)$ oscillates faster when the control $\epsilon(t)$ is large in magnitude, *vice versa*. $\int_0^t F(s) ds$ is then small in magnitude due to the mutual cancellation during the integration. Therefore, if we allow the control magnitude to be large compared to other parameters, the dissipation can be reduced remarkably.

Here we present the result of optimal control where the control range is set to $|\epsilon(t)| \leq 20\omega$ in Fig. 4.14. Note the error is smaller than the previous small range control by several orders. This is due to both phase shift correction and dissipation suppression.



(a) Z-gate error vs. operation time in a Lorentzian-like environment. Note that compared to the small range control, gate error smaller by several orders can be achieved in a much shorter operation time of $t_f \approx 0.2\omega_0^{-1}$.



(b) Z-gate error vs. operation time in an Ohmic environment, plotted at $\omega_0 t_f = 1$. Compared to Fig. 4.8, the error is much smaller even if the cutoff frequency is as high as $\omega_c = 20\omega_0$.

Figure 4.14: Results of optimal control with a large control range, $|\epsilon(t)| \leq 20\omega_0$.



Chapter 5

Conclusion

In this thesis we introduced an optimal control theory for constructing single qubit gates in an exactly solvable non-Markovian open system. The master equation of the reduced system can be exactly derived without any approximation. It is in contrast to the commonly used perturbation method, where the master equation is derived only to low orders of system-environment interaction and ignore the high order effect. Thus the dynamics derived from the perturbation method is only valid for weak system-environment coupling. The exact master equation, however, is not constrained by this limitation.

Given the exact master equation, or the equation of motion, the optimal control theory is then introduced to construct the quantum gates. Two optimization algorithms, the gradient-type method and the global improvement method, are formulated. Depending on the form of the defined final cost of the objective, appropriate optimization iteration algorithm can be applied. In our thesis, the open system dynamics is concerned, so the final cost is defined to be second order in the propagator and the gradient-type method is adopted.

We proceed to combine the exact master equation and the optimal control theory to construct the state-independent quantum gates in the presence of the Lorentzian-like

bath and the Ohmic bath. We found that for moderate qubit decay parameters, high fidelity identity gates and Z-gates can be achieved. The relation between the fidelity and the qubit decay parameters can be interpreted physically.

An important definition of improvement, Imp , is proposed to quantify how much the optimal control iteration can improve the fidelity, given that the initial guess being the ideal closed system control pulse. For an ideal closed-system, the optimal control pulse can be calculated directly. Improvement is important in that for conditions where the Imp is negligible, there is no need for optimal control and the ideal closed-system pulse suffices; on the other hand, large Imp characterizes the need for the open-system optimization iteration. We found that, mathematically, Imp is directly related to the relative magnitude of $\left| \int_0^{t_f} \text{Im}[F(s)] ds \right|$ over $\left| \int_0^{t_f} \text{Re}[F(s)] ds \right|$, and physically, it is in close relation to the shape of the spectral density with respect to the qubit transition frequency.

We further show that, for the model (dissipative model) and the control problem (σ_z control) discussed in our work, the suppression of dissipation is limited, given that we constrain the control in a relatively small range. The major improvement of gate fidelity is due to the correction to the phase shift. For control range as large as ten times of the system frequency, the dissipation can be substantially suppressed. Therefore, a system with great tunability in the transition frequency can be a good candidate of the physical implementation of this model.



Appendix A

Lorentzian spectral density and cavity QED

Consider the following summation in the continuum limit

$$\sum_{\lambda} |g_{\lambda}|^2 \rightarrow \int_0^{\infty} d\omega \rho(\omega) |g(\omega)|^2, \quad (\text{A.1})$$

where $\rho(\omega)$ is the density of states of the bath oscillators, and we define

$$D(\omega) \equiv \rho(\omega) |g(\omega)|^2 \quad (\text{A.2})$$

to be the spectral density of the reservoir.

If we consider the spectral density to be Lorentzian

$$D(\omega) = \frac{\Omega_0^2}{2\pi} \frac{\Gamma}{(\omega - \omega_c)^2 + \left(\frac{\Gamma}{2}\right)^2}, \quad (\text{A.3})$$

and the bath correlation function is then

$$\begin{aligned}
\sum_{\lambda} |g_{\lambda}|^2 e^{-i\omega_{\lambda}(t-s)} &\rightarrow \int_0^{\infty} d\omega \rho(\omega) |g(\omega)|^2 e^{-i\omega_{\lambda}(t-s)} = \int_0^{\infty} d\omega D(\omega) e^{-i\omega(t-s)} \\
&= \frac{\Omega_0^2}{2\pi} e^{-i\omega_c(t-s)} \int_{-\omega_c}^{\infty} d(\omega - \omega_c) \frac{\Gamma}{(\omega - \omega_c)^2 + \left(\frac{\Gamma}{2}\right)^2} e^{-i(\omega - \omega_c)(t-s)} \\
&\approx \frac{\Omega_0^2}{2\pi} e^{-i\omega_c(t-s)} \int_{-\infty}^{\infty} d\omega' \frac{\Gamma}{\omega'^2 + \left(\frac{\Gamma}{2}\right)^2} e^{-i\omega'(t-s)} \\
&= \Omega_0^2 e^{-\frac{\Gamma}{2}(t-s) - i\omega_c(t-s)},
\end{aligned}$$

where we have assumed that ω_c is sufficiently larger than $\frac{\Gamma}{2}$, the width of the Lorentzian function. Following the pseudo-mode method [27], we arrive at a master equation which is identical to the master equation of Jaynes-Cummings model with Damping.

Pseudo-mode master equation [with the spectral density given by Eq. (A.3)]:

$$\begin{aligned}
H_0 &= \omega_0 \sigma_+ \sigma_- + \omega_c a^{\dagger} a + \Omega_0 (a^{\dagger} \sigma_- + a \sigma_+) \\
\dot{\rho}_t &= -i [H_0, \rho_t] - \frac{\Gamma}{2} [a^{\dagger} a \rho_t - 2a \rho_t a^{\dagger} + \rho_t a^{\dagger} a]
\end{aligned}$$

where a and a^{\dagger} are the pseudo-mode operators, and ρ_t is the density operator for the composite system of atom and pseudo-mode.

Damped Jaynes-Cummings model master equation[28]:

$$\begin{aligned}
H_{\text{JCM}} &= \omega_0 \sigma_+ \sigma_- + \Omega a^{\dagger} a + g (a^{\dagger} \sigma_- + a \sigma_+) \\
\dot{\rho}_t &= -i [H_{\text{JCM}}, \rho_t] - \frac{\omega_0}{Q} [a^{\dagger} a \rho_t - 2a \rho_t a^{\dagger} + \rho_t a^{\dagger} a]
\end{aligned}$$

where ω_0 and Ω are the two-level system transition frequency and the cavity mode frequency, g is the system-cavity coupling strength, and $\frac{\omega_0}{Q}$ denotes the cavity loss rate with Q being the quality factor of the cavity.

These two master equations are identical apart from some matching of the parameters. So we can conclude that the dissipative system with a Lorentzian reservoir spectral density Eq. (A.3) physically describes the coupling of a two-level system to a single mode lossy cavity which in turn couples to a broad-band harmonic oscillator bath in vacuum state.



Appendix B

Fidelity in Closed and Open Systems

The dynamics in a closed quantum system is governed by unitary evolution

$$|\psi_t\rangle = U |\psi_0\rangle, \quad (\text{B.1})$$

where U is an unitary operator. We proceed to prove the following identity.

$\text{Re}(\text{Tr}U^\dagger V) \leq N^2$. U, V are unitary and $U, V \in \mathbb{C}^{N \times N}$.

proof.

U, V unitary,

$$\Rightarrow \begin{cases} \sum_{\alpha} U_{i\alpha} U_{j\alpha}^* = \delta_{ij} \\ \sum_{\alpha} V_{i\alpha} V_{j\alpha}^* = \delta_{ij} \end{cases} \quad (\text{B.2})$$

and

$$\begin{cases} \sum_{\alpha} U_{\alpha i} U_{\alpha j}^* = \delta_{ij} \\ \sum_{\alpha} V_{\alpha i} V_{\alpha j}^* = \delta_{ij} \end{cases} \quad (\text{B.3})$$



$$\text{Tr} [U^\dagger V] = \sum_{\alpha i} U_{i\alpha}^\dagger V_{\alpha i} = \sum_{\alpha i} U_{\alpha i}^* V_{\alpha i} \quad (\text{B.4})$$

By Cauchy-Schwarz inequality,

$$|\text{Tr} [U^\dagger V]| = \left| \sum_{\alpha i} U_{\alpha i}^* V_{\alpha i} \right|^2 \leq \sum_{\alpha i} |U_{\alpha i}|^2 \cdot \sum_{\beta j} |V_{\beta j}|^2 \quad (\text{B.5})$$

From Eq. (B.3) we have

$$\sum_{\alpha i} |U_{\alpha i}|^2 = \sum_{\beta j} |V_{\beta j}|^2 = N \quad (\text{B.6})$$

$$\therefore |\text{Tr} [U^\dagger V]| \leq N \quad (\text{B.7})$$

■

The equality in Eq. (B.7) holds when U and V are linearly dependent, *i.e.*, $X = aY$. However, for both U and V to be unitary, a must be of unit modulus. So $a = e^{i\theta}$.

This identity gives us an inspiration on the definition of closed system gate fidelity.

We may define

$$\mathcal{F} \equiv \frac{1}{N} \text{Re} \left(\text{Tr} [O^\dagger U(T)] \right) \quad (\text{B.8})$$

where O is the target and $U(T)$ is the propagator after operation time T . This definition of fidelity ensures that \mathcal{F} be in the range $[0, 1]$ and reaches its maximum when O and $U(T)$ only differs by a global phase.

In open systems, the evolution is no longer unitary. The definition in Eq. (B.8) does not provide enough information on quantifying the distance between two matrices. We define the gate error by

$$\begin{aligned} J_T &\equiv \frac{1}{2N} \text{Tr} \left\{ (O - \mathcal{G}(T))^\dagger (O - \mathcal{G}(T)) \right\} \\ &= \frac{1}{2N} \sum_{ij} |(O - \mathcal{G}(T))_{ij}|^2 \end{aligned} \quad (\text{B.9})$$

which is always positive unless $\mathcal{G}(T)$ is identically equal to the target O . And the

fidelity is defined to be $1 - J_T$.

When the dynamics is unitary, namely $\mathcal{G}(T)$ is unitary, J_T becomes

$$\begin{aligned}
 J_T &= \frac{1}{2N} \text{Tr} \left\{ \underbrace{O^\dagger O}_I - O^\dagger \mathcal{G}(T) - \mathcal{G}^\dagger(T) O + \underbrace{\mathcal{G}^\dagger(T) \mathcal{G}(T)}_I \right\} \\
 &= \frac{1}{2N} \left\{ \text{Tr}[2I] - 2\text{Re} \left(\text{Tr} [O^\dagger \mathcal{G}(T)] \right) \right\} \\
 &= 1 - \frac{1}{N} \text{Re} \left(\text{Tr} [O^\dagger \mathcal{G}(T)] \right)
 \end{aligned} \tag{B.10}$$


Thus the fidelity in open systems $\mathcal{F} = 1 - J_T$ reduces to the same form as in the closed system.

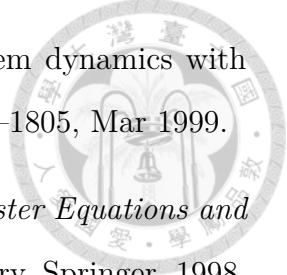




Bibliography

- [1] L. Diósi, N. Gisin, and W. T. Strunz. Non-markovian quantum state diffusion. *Phys. Rev. A*, 58:1699–1712, Sep 1998.
- [2] R. P. Feynman. Simulating Physics with Computers. *International Journal of Theoretical Physics*, 21:467–488, June 1982.
- [3] P. W. Shor. Polynomial-Time Algorithms for Prime Factorization and Discrete Logarithms on a Quantum Computer. *SIAM Review*, 41:303–332, January 1999.
- [4] Lov K. Grover. A fast quantum mechanical algorithm for database search. In *Proceedings of the twenty-eighth annual ACM symposium on Theory of computing*, STOC '96, pages 212–219, New York, NY, USA, 1996. ACM.
- [5] J. I. Cirac and P. Zoller. Quantum computations with cold trapped ions. *Phys. Rev. Lett.*, 74:4091–4094, May 1995.
- [6] D. Jaksch, C. Bruder, J. I. Cirac, C. W. Gardiner, and P. Zoller. Cold bosonic atoms in optical lattices. *Phys. Rev. Lett.*, 81:3108–3111, Oct 1998.
- [7] Yuriy Makhlin, Gerd Schön, and Alexander Shnirman. Quantum-state engineering with josephson-junction devices. *Rev. Mod. Phys.*, 73:357–400, May 2001.
- [8] L. Childress, M. V. G. Dutt, J. M. Taylor, A. S. Zibrov, F. Jelezko, J. Wrachtrup, P. R. Hemmer, and M. D. Lukin. Coherent Dynamics of Coupled Electron and Nuclear Spin Qubits in Diamond. *Science*, 314:281–285, October 2006.

- 
- [9] B. E. Kane. A silicon-based nuclear spin quantum computer. *Nature*, 393(6681):133–137, May 1998.
- [10] P. Rebentrost, I. Serban, T. Schulte-Herbrüggen, and F. K. Wilhelm. Optimal control of a qubit coupled to a non-markovian environment. *Phys. Rev. Lett.*, 102:090401, Mar 2009.
- [11] M. Wenin and W. Pötz. Minimization of environment-induced decoherence in quantum subsystems and application to solid-state-based quantum gates. *Phys. Rev. B*, 78:165118, Oct 2008.
- [12] Jens Clausen, Guy Bensky, and Gershon Kurizki. Bath-optimized minimal-energy protection of quantum operations from decoherence. *Phys. Rev. Lett.*, 104:040401, Jan 2010.
- [13] Jacob R. West, Daniel A. Lidar, Bryan H. Fong, and Mark F. Gyure. High fidelity quantum gates via dynamical decoupling. *Phys. Rev. Lett.*, 105:230503, Dec 2010.
- [14] V.F. Krotov. *Global Methods in Optimal Control Theory*. Chapman and Hall/CRC Pure and Applied Mathematics Series. MARCEL DEKKER Incorporated, 1996.
- [15] R. Clifton. *Perspectives on quantum reality: non-relativistic, relativistic, and field-theoretic*. University of Western Ontario series in philosophy of science. Kluwer Academic Publishers, 1996.
- [16] I. Percival. *Quantum State Diffusion*. Cambridge University Press, 1998.
- [17] Lajos Diósi and Walter T. Strunz. The non-markovian stochastic schrodinger equation for open systems. *Physics Letters A*, 235(6):569 – 573, 1997.
- [18] Lajos Diósi, Nicolas Gisin, Jonathan Halliwell, and Ian C. Percival. Decoherent histories and quantum state diffusion. *Phys. Rev. Lett.*, 74:203–207, Jan 1995.

- 
- [19] Walter T. Strunz, Lajos Diósi, and Nicolas Gisin. Open system dynamics with non-markovian quantum trajectories. *Phys. Rev. Lett.*, 82:1801–1805, Mar 1999.
- [20] H.J. Carmichael. *Statistical Methods in Quantum Optics 1: Master Equations and Fokker-Planck Equations*. Physics and Astronomy Online Library. Springer, 1998.
- [21] Walter T. Strunz. Linear quantum state diffusion for non-markovian open quantum systems. *Physics Letters A*, 224(1):25 – 30, 1996.
- [22] L.C. Young. *Lectures on the Calculus of Variations and Optimal Control Theory*. 1969.
- [23] M. Athans and P.L. Falb. *Optimal Control: An Introduction to the Theory And Its Applications*. Dover Books on Engineering Series. DOVER PUBN Incorporated, 2006.
- [24] Shlomo E. Sklarz and David J. Tannor. Loading a bose-einstein condensate onto an optical lattice: An application of optimal control theory to the nonlinear schrödinger equation. *Phys. Rev. A*, 66:053619, Nov 2002.
- [25] M.A. Nielsen and I.L. Chuang. *Quantum Computation and Quantum Information*. Cambridge Series on Information and the Natural Sciences. Cambridge University Press, 2000.
- [26] A. J. Leggett, S. Chakravarty, A. T. Dorsey, Matthew P. A. Fisher, Anupam Garg, and W. Zwerger. Dynamics of the dissipative two-state system. *Rev. Mod. Phys.*, 59:1–85, Jan 1987.
- [27] B. M. Garraway. Nonperturbative decay of an atomic system in a cavity. *Phys. Rev. A*, 55:2290–2303, Mar 1997.
- [28] Bruce W. Shore and Peter L. Knight. The jaynes-cummings model. *Journal of Modern Optics*, 40(7):1195–1238, 1993.